Supporting Information

Enzymatic Peptide Macrocyclization via Indole-*N*-Acylation

Hiroto Maruyama[1], Yuito Yamada[1], Yasuhiro Igarashi[2], Kenichi Matsuda*[1], Toshiyuki Wakimoto*[1]

[1]Faculty of Pharmaceutical Science, Hokkaido University, Kita 12, Kita-ku, Sapporo, 060-0812, Japan

[2]Biotechnology Research Center and Department of Biotechnology, Toyama Prefectural University, 5180 Kurokawa, Imizu, Toyama, 939-0398, Japan

Table of Contents

General remarks

^{1}H and ^{13}C NMR spectra were recorded on a JEOL ECZ 500 R (500 MHz for ^{1}H NMR) or a JEOL ECZ 400 (400 MHz for ^{1}H NMR) spectrometer. Chemical shifts are denoted in δ (ppm) relative to residual solvent peaks as internal standard (DMSO-d_6, ^{1}H δ 2.50, ^{13}C δ 39.5). ESI-MS spectra were recorded on a SHIMADZU LCMS-2050 spectrometer, a Thermo Scientific Exactive mass spectrometer, and an amaZon SL-NPC (Bruker Daltonics). High performance liquid chromatography (HPLC) experiments were performed with a SHIMADZU HPLC system equipped with a LC-2050C 3D intelligent pump. All reagents were used as supplied unless otherwise stated. Oligonucleotides used for genetic manipulation were purchased from Fasmac Co., Ltd. (Kanagawa, Japan). Protein structure prediction was performed by AlphaFold2 [1] with parameters set at default.

Construction of expression plasmid of BulbE-TE

pET28a (EMD Millipore) was used as an expression vector. BulbE-TE-pET28a (GenBank: WHI53517.1), an expression plasmid for BulbE-TE with His6-tag fused at its *N*-terminus, was Codon-optimized and synthesized by Twist Bioscience.

Construction of expression plasmids of BulbE-TE mutants (C731S, E732Q, T822I, T824L)

The DNA fragments coding for BulbE-TE mutants were amplified by KOD One® PCR Master Mix -Blue- (TOYOBO), using a set of primers listed in Table S1. BulbE-TE-pET28a was used as a template.

Enzyme expression and purification

50 μg/ml kanamycin were used for the selection of *E. coli* host harboring pET28a-based plasmids. The expression plasmids were introduced into *E. coli* BL21 (DE3) and a single colony was inoculated into 5 mL of 2xYT media (1.6% Bacto tryptone, 1.0% Bact yeast extract, 0.5% NaCl) containing 50 μg/ml kanamycin and was cultured at 37 °C for overnight as seed culture. 2.0 mL of cultural broth was transferred to 200 mL of 2xYT media containing 50 μg/ml kanamycin and culture at 37 °C for three hours. The broth was cooled on ice and 0.1 mM of IPTG (isopropyl β-D-thiogalactopyranoside) was added to induce the expression of recombinant enzymes. *E. coli* was cultured at 16 °C for overnight. Cell was washed with lysis buffer (20 mM Tris-HCl pH8.0, 150 mM NaCl), then successively homogenized by sonication. Cell debris were precipitated by centrifugation with 20,380 × *g* for 10 min at 4 °C, then the supernatant was subjected to TALON® Metal Affinity resin (Takara), which was equilibrated by wash buffer (20 mM Tris-HCl pH8.0, 150 mM NaCl, 40 mM imidazole pH8.0). The column was washed with an additional wash buffer, then eluted with elution buffer (20 mM Tris-HCl pH8.0, 150 mM NaCl, 200 mM imidazole pH8.0). Imidazole was removed by an Amicon Ultra 4 ml filter (Merck Millipore). The concentrations of proteins were measured using a Bio-Rad protein assay kit (Bio-Rad).

In vitro reactions

50 μL of reaction mixture containing 50 mM Tris-HCl (pH 8.0), 50 mM EDTA (pH 8.0), and 200 μM acyclic precursor was prepared. Reaction was initiated by the addition of 20 μM BulbE TE, then the mixture was incubated at 25 °C for 12 h. Reaction was quenched by adding equal volume of MeOH, and centrifuged at 20,380 × *g* for 10 min. The supernatant was analyzed by LC-MS or HPLC.

LC-MS and HPLC analysis

Analytical conditions used in this study are listed in Table S5. The concentration of enzymatic products was estimated based on the extinction coefficient ε (210 nm), which was determined experimentally. ε (210 nm) values were assumed to be equal for substrate and corresponding enzymatic products.

LC-MS/MS analysis

Samples were separated with a SHIMADZU HPLC system equipped with a LC-20AD intelligent pump. The HPLC system was operated in analytical condition 4 described in Table S5. LC-MS/MS experiments were performed with amaZon SL-NPC (Bruker Daltonics). Fragmentation of precursor ions were also performed with amaZon SL-NPC using helium gas with amplitude value 1.0 V.

General procedure for solid-phase peptide synthesis (SPPS).

Step 1: Fmoc group of the solid supported peptide was removed by using 20% piperidine/DMF (10 min, room temperature).

Step 2: The resin in the reaction vessel was washed with DMF (×3) and CH_2Cl_2 (×3).

Step 3: To the solution of Fmoc-protected building blocks (4 eq) were added DIC (4 eq in NMP) and Oxyma (4 eq in DMF). After 2~3 min of pre-activation, the mixture was injected to the reaction vessel. The resulting mixture was mixed for 15 min at 60 °C

Step 4: The resin in the reaction vessel was washed with DMF (×3) and CH_2Cl_2 (×3). Amino acids were condensed onto the solid support by repeating Step 1-4.

Synthesis of SNAC peptides (**2**, **9-18**)

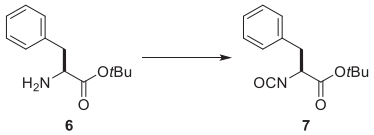

***(S)-t*-Butyl-2-isocyanato-3-phenylpropanate (7):** L-phenylalanine *t*-butyl ester (**6**) (776.75 mg, 3.01 mmol) and saturated aqueous $NaHCO_3$ (10 mL) was added in CH_2Cl_2 (10 mL) and cooled in an ice bath. Triphosgene (302.25 mg, 1.02 mmol) was added, and stirred in the ice bath for 15 min. This reaction mixture was extracted with CH_2Cl_2 (3 times). The organic layer was washed with brine, dried over Na_2SO_4, and filtered. The solvent was removed in vacuo to give **7** (177.4 mg, 24%), which was used in the next reaction without further purification. The analytical data of **7** were identical to those reported previously [2]. [CAS 117156-31-7]

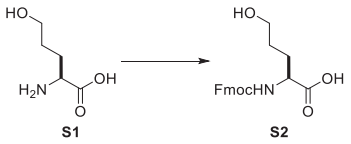

***(S)-N*-Fmoc-5-hydroxy-norvaline (S2):** To a solution of *(S)*-5-hydroxy-norvaline(**S1**) (138.0 mg, 1.04 mmol) in aqueous 10% $NaHCO_3$ (3 mL) was cooled in an ice bath. a solution of fluorenyl methoxycarbonyl chloride (311.0 mg, 1.20 mmol) in 1,4-dioxane (3 mL) was slowly added, and stirred for 2 h at room temperature. This reaction mixture was washed with AcOEt, added 1M HCl, and extracted with AcOEt. The organic layer was washed with brine, dried over Na_2SO_4, and filtered. The solvent was removed in vacuo to give **S2** (313.0 mg, 88%), which was used in the next reaction without further purification. The analytical data of **S2** were identical to those reported previously [3]. [CAS 2169956-19-6]

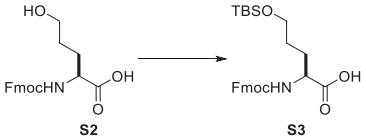

***(S)-N*-Fmoc-5-*t*-butyldimetylsilyloxy-norvaline (S3): S2** (313.0 mg, 0.92 mmol) and imidazole (224.3 mg, 3.30 mmol) were added in THF (6 mL) and stirred for 5 min. TBSCl (452.2 mg, 3.00 mmol) was added, and stirred for 24 h at room temperature. Then, saturated aqueous NH_4Cl was added, and extracted with AcOEt (3 times). The organic layer was washed with brine, dried over Na_2SO_4, and filtered. The solvent was removed in vacuo, and the crude product was purified by column chromatography on silica gel (Hexane:AcOEt = 1:1) to give to **S3** (429.2 mg, quant). The analytical data of **S3** were identical to those reported previously [3]. [CAS 212388-38-0]

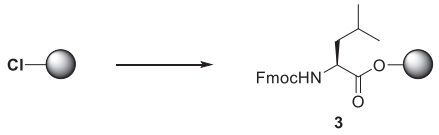

3

Fmoc-L-Leu-2-chlorotrityl resin (3): 2-chlorotrityl resin (87.4 mg, 0.11 mmol) in Libra tube was swelled with CH_2Cl_2 for 10 min, and then the excess solvent was removed by filtration. To the resin was added a solution of Fmoc-L-Leu-OH (146.8 mg, 0.10 mmol) and *i*-Pr_2NEt (50 μL, 0.15 mmol) in CH_2Cl_2 (0.5 mL), and shaken for 2 h at 37 °C. After the reaction mixture was filtered, washed with DMF (×3) and CH_2Cl_2 (×3) to give Fmoc-L-Leu-2-chlorotrityl resin (**3**).

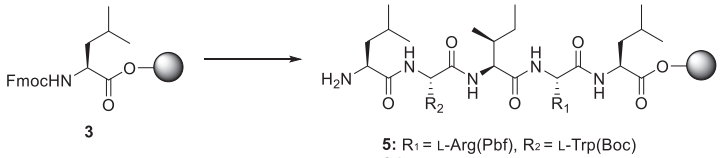

5: R_1 = L-Arg(Pbf), R_2 = L-Trp(Boc)
S4: R_1 = L-Arg(Pbf), R_2 = L-Orn(Boc)
S5: R_1 = L-Arg(Pbf), R_2 = L-Ser(*t*Bu)
S6: R_1 = L-Arg(Pbf), R_2 = L-Nva(5-OTBS)
S7: R_1 = L-Arg(Pbf), R_2 = L-Tyr(*t*Bu)
S8: R_1 = L-Arg(Pbf), R_2 = L-His(Trt)
S9 R_1 = L-Arg(Pbf), R_2 = L-Arg(Pbf)
S10: R_1 = L-Arg(Pbf), R_2 = L-Gln(Trt)
S11: R_1 = L-Glu(*t*Bu), R_2 = L-Trp(Boc)

Pentapeptide-2-chlorotrityl resins (5, S4-S11): The resin **3** in Libra tube were swelled in DMF for 10 min, which was subjected to 4 cycles [**5**: Fmoc-L-Arg(Pbf)-OH, Fmoc-L-Ile-OH, Fmoc-L-Trp(Boc)-OH, Fmoc-L-Leu-OH, **S4**: Fmoc-L-Arg(Pbf)-OH, Fmoc-L-Ile-OH, Fmoc-L-Orn(Boc)-OH, Fmoc-L-Leu-OH, **S5**: Fmoc-L-Arg(Pbf)-OH, Fmoc-L-Ile-OH, Fmoc-L-Ser(*t*Bu)-OH, Fmoc-L-Leu-OH, **S6**: Fmoc-L-Arg(Pbf)-OH, Fmoc-L-Ile-OH, **S3**, Fmoc-L-Leu-OH, **S7**: Fmoc-L-Arg(Pbf)-OH, Fmoc-L-Ile-OH, Fmoc-L-Tyr(*t*Bu)-OH, Fmoc-L-Leu-OH, **S8**: Fmoc-L-Arg(Pbf)-OH, Fmoc-L-Ile-OH, Fmoc-L-His(Trt)-OH, Fmoc-L-Leu-OH, **S9**: Fmoc-L-Arg(Pbf)-OH, Fmoc-L-Ile-OH, Fmoc-L-Arg(Pbf)-OH, Fmoc-L-Leu-OH, **S10**: Fmoc-L-Arg(Pbf)-OH, Fmoc-L-Ile-OH, Fmoc-L-Gln(Trt)-OH, Fmoc-L-Leu-OH, **S11**: Fmoc-L-Glu(*t*Bu)-OH, Fmoc-L-Ile-OH, Fmoc-L-Trp(Boc)-OH, Fmoc-L-Leu-OH] of SPPS protocol described above (p4, Step1-4) to afford pentapeptide-2-chlorotrityl resins (**5, S4-S11)**.

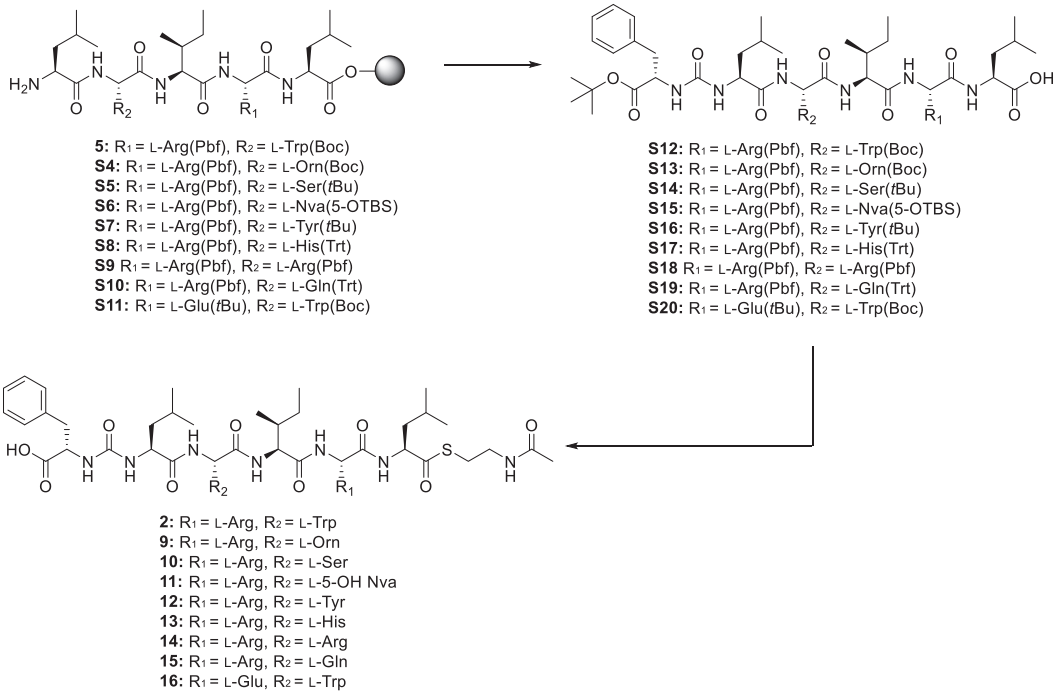

5: R_1 = L-Arg(Pbf), R_2 = L-Trp(Boc)
S4: R_1 = L-Arg(Pbf), R_2 = L-Orn(Boc)
S5: R_1 = L-Arg(Pbf), R_2 = L-Ser(*t*Bu)
S6: R_1 = L-Arg(Pbf), R_2 = L-Nva(5-OTBS)
S7: R_1 = L-Arg(Pbf), R_2 = L-Tyr(*t*Bu)
S8: R_1 = L-Arg(Pbf), R_2 = L-His(Trt)
S9 R_1 = L-Arg(Pbf), R_2 = L-Arg(Pbf)
S10: R_1 = L-Arg(Pbf), R_2 = L-Gln(Trt)
S11: R_1 = L-Glu(*t*Bu), R_2 = L-Trp(Boc)

S12: R_1 = L-Arg(Pbf), R_2 = L-Trp(Boc)
S13: R_1 = L-Arg(Pbf), R_2 = L-Orn(Boc)
S14: R_1 = L-Arg(Pbf), R_2 = L-Ser(*t*Bu)
S15: R_1 = L-Arg(Pbf), R_2 = L-Nva(5-OTBS)
S16: R_1 = L-Arg(Pbf), R_2 = L-Tyr(*t*Bu)
S17: R_1 = L-Arg(Pbf), R_2 = L-His(Trt)
S18 R_1 = L-Arg(Pbf), R_2 = L-Arg(Pbf)
S19: R_1 = L-Arg(Pbf), R_2 = L-Gln(Trt)
S20: R_1 = L-Glu(*t*Bu), R_2 = L-Trp(Boc)

2: R_1 = L-Arg, R_2 = L-Trp
9: R_1 = L-Arg, R_2 = L-Orn
10: R_1 = L-Arg, R_2 = L-Ser
11: R_1 = L-Arg, R_2 = L-5-OH Nva
12: R_1 = L-Arg, R_2 = L-Tyr
13: R_1 = L-Arg, R_2 = L-His
14: R_1 = L-Arg, R_2 = L-Arg
15: R_1 = L-Arg, R_2 = L-Gln
16: R_1 = L-Glu, R_2 = L-Trp

SNAC-substrates (2, 9-16): The resins **5** and **S4-S11** in Libra tubes were swelled in CH_2Cl_2 for 10 min, and then the excess solvents were removed by filtration. To the resins were added a solution of **7** (98.8 mg, 0.40 mmol) and *i*-Pr_2NEt (50 μL, 0.15 mmol) in CH_2Cl_2 (0.5 mL), and shaken for 2 h at 40 °C. After the reaction mixtures were filtered, washed with DMF (×3) and CH_2Cl_2 (×3), added HFIP/CH_2Cl_2 =3:7 (1.0 mL), shaken for 30 min, and filtered. These procedures were repeated 2 times to give ureido containing peptapeptides (**S12-S20**). **S12-S20** were used in the next reactions without further purification. To ureido containing peptapeptides **S12-S20** in DMF (1 mL) were added PyBOP (104.2 mg, 0.20 mmol) and SNAC (22 μL, 0.20 mmol). After being stirred for 30 min at – 20 °C, added 2,6-lutidine (11 μL, 0.10 mmol) and stirred overnight at room temperature. The reaction mixtures were concentrated, and the peptides diluted with AcOEt and aqueous NH_4Cl. The resulting mixtures were extracted with AcOEt (×3), washed with brine, dried over Na_2SO_4 and concentrated. The residues were added TFA/phenol/*i*-Pr_3SiH/DODT =92.5:2.5:2.5:2.5 (3.0 mL). After Stirred for 2 h, the resulting mixtures were diluted with Et_2O (30 mL) and chilled (–80 ℃), then centrifuged with 3,500 × *g* for 10 min at 4 ℃ to afford crude peptides. The crude peptides were purified by HPLC analytical condition 1 described in Table S5, to afford SNAC-substrate **2** (13.1 mg, 13.3% for 13 steps), **9** (13.1 mg, 13.3% for 13 steps), **10** (15.6 mg, 17.4% for 13 steps), **11** (2.1 mg, 2.3% for 13 steps), **12** (19.7 mg, 20.3% for 13 steps), **13** (10.2 mg, 10.8% for 13 steps), **14** (27.6 mg, 28.7% for 13 steps), **15** (18.9 mg, 20.2% for 13 steps), **16** (9.1 mg, 9.9% for 13 steps).

seco-bulbiferamide-SNAC (**2**): ^{1}H NMR (400 MHz, DMSO-d_6): δ 10.73 (s, 1H), 8.50 (d, *J*= 6.4 Hz, 1H), 8.09-8.01 (m, 3H), 7.94 (d, *J*= 6.4 Hz, 1H), 7.75-7.65 (m, 2H), 7.57-6.74 (m, 4H), 7.27 (d, *J*= 6.4 Hz, 2H), 7.22 (t, *J*= 6.0 Hz, 1H), 7.15 (t, *J*= 5.6 Hz, 2H), 7.08 (s, 1H), 7.01 (t, *J*= 5.6 Hz, 1H), 6.91 (t, *J*= 5.6 Hz, 1H), 6.32 (br, 1H), 6.17 (br, 1H), 4.56 (q, *J*= 4.4 Hz, 1H), 4.32 (br, 3H), 4.20 (t, *J*= 6.0 Hz, 1H), 4.06 (br, 1H), 3.62-2.30 (m, 11H), 1.80-0.94 (m, 15H), 0.84-0.71 (m, 18H); ^{13}C NMR (100 MHz, DMSO-d_6): δ 201.9, 174.3, 173.6, 172.2, 171.7, 171.1, 170.0, 157.7, 157.2, 137.8, 136.5, 129.8, 129.8, 128.7, 128.7, 125.0, 123.9, 121.3, 119.6, 118.9, 118.7, 110.5, 110.1, 58.0, 57.2, 54.4, 53.6, 52.5, 52.2, 46.4, 46.4, 42.6, 42.5, 38.0, 38.0, 37.5, 28.2, 26.4, 26.4, 25.6, 24.7, 24.5, 23.6, 23.5, 23.0, 22.3, 21.4, 15.6, 11.6; HRMS (ESI) calcd for $C_{49}H_{74}N_{11}O_9S^+$ $[M+H]^+$ 992.53.66, found 992.53972.

seco-bulbiferamide(W3O)-SNAC (**9**): ^{1}H NMR (400 MHz, DMSO-d_6): δ 8.53 (d, *J*= 7.6 Hz, 1H), 8.13 (d, *J*= 7.6 Hz, 1H), 8.08-7.96 (m, 3H), 7.57 (t, *J*= 8.4 Hz, 1H), 7.57-6.74 (m, 4H), 7.26-7.12 (m, 4H), 6.31 (d, *J*= 7.6 Hz, 1H), 6.21 (d, *J*= 8.4 Hz, 1H), 4.40-4.21 (m, 6H), 3.28-2.30 (m, 15H), 1.80-0.94 (m, 17H), 0.84-0.71 (m, 18H); ^{13}C NMR (100 MHz, DMSO-d_6): δ 201.9, 174.3, 173.8, 172.3, 171.5, 170.0, 170.0, 157.7, 157.2, 137.8, 129.8, 129.8, 128.7, 128.7, 127.2, 58.0, 57.3, 54.8, 52.3, 52.2, 52.2, 47.2, 45.9, 44.9, 42.7, 40.9, 39.0, 38.6, 38.0, 28.2, 25.7, 24.6, 24.5, 24.1, 23.7, 23.7, 23.5, 23.0, 22.4, 22.4, 21.4, 15.7, 11.7; HRMS (ESI) calcd for $C_{43}H_{74}N_{11}O_9S^+$$[M+H]^+$ 920.53812, found 920.53972.

seco-bulbiferamide(W3S)-SNAC (**10**): ^{1}H NMR (500 MHz, DMSO-d_6): δ 8.45 (d, *J*= 8.0 Hz, 1H), 8.07-7.97 (m, 4H), 7.54 (d, *J*= 9.0 Hz, 1H), 7.10-6.54 (m, 4H), 7.26-7.12, (m, 4H), 6.45 (d, *J*= 8.0 Hz, 1H), 6.22 (d, *J*= 7.0 Hz, 1H), 4.52 (q, *J*= 7.0 Hz, 1H), 4.36-4.22 (m, 4H), 4.22-4.17 (m, 1H), 4.14-4.08 (m, 1H), 3.28-2.30 (m, 11H), 1.80-0.94 (m, 15H), 0.84-0.71 (m, 18H); ^{13}C NMR (125 MHz, DMSO-d_6): δ 201.9, 174.2, 173.8, 172.2, 171.1, 170.4, 170.0, 157.7, 157.3, 137.8, 129.8, 129.8, 128.7, 128.7, 127.0, 61.8, 58.0, 57.3, 55.4, 54.4, 52.5, 52.1, 46.4, 45.3, 42.5, 38.6, 38.0, 37.4, 37.0, 28.2, 25.6, 24.6, 24.6, 24.1, 23.6, 23.5, 23.0, 22.3, 21.4, 15.7, 11.8; HRMS (ESI) calcd for $C_{41}H_{68}N_{10}O_{10}SNa^+$$[M+Na]^+$ 915.47196, found 915.47438.

seco-bulbiferamide(W3Nva5-OH)-SNAC (**11**): ^{1}H NMR (500 MHz, DMSO-d_6): δ 8.49 (d, *J*= 7.5 Hz, 1H), 8.09-7.94 (m, 4H), 7.56 (d, *J*= 8.5 Hz, 1H), 7.47-6.74 (m, 4H), 7.23 (t, *J*= 6.0 Hz, 2H), 7.15 (d, *J*= 7.0 Hz, 2H), 6.32 (d, *J*= 7.5 Hz, 1H), 6.17 (d, *J*= 8.0 Hz, 1H), 4.43-4.05 (m, 7H), 3.46-2.75 (m, 11H), 1.80-0.94 (m, 19H), 0.88-0.71 (m, 18H); ^{13}C NMR (125 MHz, DMSO-d_6): δ 201.9, 174.2, 173.5, 172.2, 171.4, 171.2, 169.9, 157.6, 157.2, 137.8, 129.8, 129.8, 128.7, 128.7, 126.9, 60.9, 58.0, 57.0, 54.5, 53.0, 52.9, 52.7, 52.4, 51.9, 42.7, 42.6, 41.5, 38.6, 38.0, 37.4, 29.3, 28.2, 25.6, 25.5, 24.6, 23.6, 23.5, 23.0, 22.5, 21.9, 21.4, 15.7, 11.6; HRMS (ESI) calcd for $C_{43}H_{72}N_{10}O_{10}SNa^+$$[M+Na]^+$ 943.50348, found 943.50568.

seco-bulbiferamide(W3Y)-SNAC (**12**): ^{1}H NMR (500 MHz, DMSO-d_6): δ 9.13 (s,1H), 8.51 (d, *J*= 7.5 Hz, 1H), 8.04 (d, *J*= 6.0 Hz, 1H),7.90 (d, *J*= 8.0 Hz, 1H), 7.67 (d, *J*= 8.0 Hz, 1H), 7.50 (d, *J*= 5.0 Hz, 1H), 7.57-6.74 (m, 4H), 7.23 (t, *J*= 7.0 Hz, 2H), 7.16 (t, *J*= 7.0 Hz, 1H), 7.13 (d, *J*= 7.0 Hz, 2H), 6.94 (d, *J*= 7.5 Hz, 2H), 6.57 (d, *J*= 7.5 Hz, 2H), 6.24 (d, *J*= 8.0 Hz, 1H), 6.17 (d, *J*= 8.0 Hz, 1H), 4.46-4.26 (m, 4H), 4.18 (br, 1H), 4.03 (br, 1H), 3.25-2.28 (m, 11H),

1.80-0.94 (m, 15H), 0.84-0.71 (m, 18H); ^{13}C NMR (125 MHz, DMSO-*d*$_6$): δ 201.9, 174.2, 173.4, 172.2, 171.4, 171.2, 170.0, 157.6, 157.3, 156.3, 137.7, 130.5, 130.5, 129.8, 129.8, 128.7, 128.7, 128.2, 126.9, 115.3, 115.3, 58.0, 57.1, 54.4, 54.4, 54.3, 52.5, 52.1, 46.4, 45.3, 42.6, 38.5, 38.0, 37.5, 36.6, 28.2, 26.4, 25.6, 24.7, 24.5, 23.6, 23.5, 23.0, 22.3, 21.4, 15.6, 11.6; HRMS (ESI) calcd for $C_{47}H_{73}N_{10}O_{10}S^+[M+H]^+$ 969.52256, found 969.52373.

seco-bulbiferamide(W3H)-SNAC (**13**): ^{1}H NMR (500 MHz, DMSO-*d*$_6$): δ 8.75 (s, 1H), 8.52 (d, *J*= 7.5 Hz, 1H), 8.31 (d, *J*= 8.0 Hz, 1H), 8.17 (d, *J*= 7.0 Hz, 1H), 8.05 (d, *J*= 5.5 Hz, 1H), 7.64 (d, *J*= 8.0 Hz, 1H), 7.75 (s, 1H), 7.57-6.74 (m, 4H), 7.23 (m, *J*= 7.0 Hz, 3H), 7.15 (d, *J*= 7.5 Hz, 2H), 6.40 (d, *J*= 7.0 Hz, 1H), 6.21 (d, *J*= 8.0 Hz, 1H), 4.56 (q, *J*= 6.0 Hz, 1H), 4.40-4.24 (m, 3H), 4.18 (t, *J*= 7.5 Hz, 1H), 4.01 (q, *J*= 7.5 Hz, 1H), 3.62-2.63 (m, 11H), 1.80-0.94 (m, 15H), 0.88-0.71 (m, 18H); ^{13}C NMR (125 MHz, DMSO-*d*$_6$): δ 201.9, 174.2, 173.9, 172.2, 171.2, 170.3, 169.9, 157.9, 157.4, 137.8, 134.2, 129.8, 129.8, 128.7, 128.7, 127.0, 117.4, 102.7, 58.0, 57.2, 54.4, 53.6, 52.5, 52.2, 42.0, 38.5, 38.5, 38.0, 37.8, 37.5, 35.8, 32.1, 28.2, 26.4, 26.4, 25.7, 24.5, 23.6, 23.5, 23.0, 22.3, 21.4, 15.6, 11.6; HRMS (ESI) calcd for $C_{44}H_{71}N_{12}O_9S^+[M+H]^+$ 943.51708, found 969.51932.

seco-bulbiferamide(W3R)-SNAC (**14**): ^{1}H NMR (500 MHz, DMSO-*d*$_6$): δ 8.50 (d, *J*= 7.5 Hz, 1H), 8.11 (d, *J*= 8.0 Hz, 1H), 8.08-8.01 (m, 3H), 7.73 (d, *J*= 5.0 Hz, 1H), 7.57-6.74 (m, 8H), 7.23 (t, *J*= 7.5 Hz, 2H), 7.15 (m, 2H), 6.35 (d, *J*= 7.5 Hz, 1H), 6.17 (d, *J*= 8.0 Hz, 1H), 4.36-4.16 (m, 5H), 4.08 (q, *J*= 5.5 Hz, 1H), 3.12-2.35 (m, 11H), 1.80-0.94 (m, 19H), 0.84-0.71 (m, 18H); ^{13}C NMR (125 MHz, DMSO-*d*$_6$): δ 201.9, 174.3, 173.8, 172.2, 171.6, 171.1, 170.0, 157.7, 157.3, 157.3, 137.9, 129.8, 129.8, 128.7, 128.7, 127.0, 58.0, 57.0, 54.6, 52.7, 52,5, 52.1, 52.0, 46.4, 46.4, 42.5, 38.6, 38.6, 38.0, 37.7, 28.2, 26.4, 26.4, 25.7, 25.6, 24.6, 24.5, 23.6, 23.5, 23.0, 22.4, 21.4, 15.6, 11.6; HRMS (ESI) calcd for $C_{44}H_{76}N_{13}O_9S^+[M+H]^+$ 962.55925, found 962.56151.

seco-bulbiferamide(W3N)-SNAC (**15**): ^{1}H NMR (400 MHz, DMSO-*d*$_6$): δ 8.48 (d, *J*= 7.5 Hz, 1H), 8.09-7.94 (m, 2H), 7.63 (d, *J*= 8.5 Hz, 1H), 7.53 (t, *J*= 5.5 Hz, 1H), 7.57-6.74 (m, 4H), 7.25 (d, *J*= 6.4 Hz, 2H), 7.24 (t, *J*= 6.0 Hz, 1H), 7.15 (t, *J*= 5.6 Hz, 2H), 6.78 (s, 2H), 6.32 (d, *J*= 7.5 Hz, 1H), 6.19 (d, *J*= 7.0 Hz, 1H), 4.56 (q, *J*= 7.0 Hz, 1H), 4.35-4.24 (m, 3H), 4.17 (q, *J*= 7.0 Hz, 1H), 4.07 (br, 1H), 3.17-2.40 (m, 13H), 1.80-0.94 (m, 15H), 0.84-0.71 (m, 18H); ^{13}C NMR (100 MHz, DMSO-*d*$_6$): δ 201.9, 174.6, 174.3, 173.7, 172.3, 171.6, 171.3, 170.0, 157.7, 157.2, 137.8, 129.8, 129.8, 128.7, 128.7, 127.0, 58.0, 57.0, 54.5, 52.6, 52.5, 52.0, 42.6, 38.6, 38.6, 38.0, 37,3, 37.0, 32.0, 29.3, 28.2, 28.0, 25.6, 24.6, 24.6, 24.5, 23.6, 23.5, 23.0, 22.4, 21.3, 15.7, 11.6; HRMS (ESI) calcd for $C_{43}H_{71}N_{11}O_{10}SNa^+[M+Na]^+$ 956.49890, found 956.500093.

seco-bulbiferamide(R5E)-SNAC (**16**): ^{1}H NMR (500 MHz, DMSO-*d*$_6$): δ 10.69 (s, 1H), 8.48 (d, *J*= 7.5 Hz, 1H), 8.09-8.01 (m, 3H), 7.76 (d, *J*= 8.5 Hz, 1H), 7.50 (d, *J*= 7.5 Hz, 2H), 7.26 (d, *J*= 8.0 Hz, 2H), 7.22 (t, *J*= 7.5 Hz, 1H), 7.13 (t, *J*= 7.0 Hz, 2H), 7.06 (s, 1H), 6.99 (t, *J*= 7.0 Hz, 1H), 6.90 (t, *J*= 7.5 Hz, 1H), 6.29 (d, *J*= 8.0 Hz, 1H), 6.17 (d, *J*= 8.0 Hz, 1H), 4.54 (q, *J*= 5.0 Hz, 1H), 4.32-4.01 (m, 5H), 3.62-2.30 (m, 9H), 1.80-0.94 (m, 15H), 0.84-0.71 (m, 18H); ^{13}C NMR (125 MHz, DMSO-*d*$_6$): δ 201.9, 174.5, 174.2, 173.5, 172.0, 171.7, 171.2, 169.8, 157.6, 137.8, 136.5, 129.8, 129.8, 128.7, 128.7, 127.9, 126.9, 123.9, 121.3, 118.9, 118.7, 111.7, 110.5, 58.0, 57.2, 54.4, 53.6, 52.2, 52.0, 42.7, 38.7, 38.7, 38.0, 37.4, 30.7, 28.2, 27.6, 27.5, 24.7, 24.5, 23.7, 23.4, 23.4, 23.0, 22.3, 21.4, 15.6, 11.6; HRMS

(ESI) calcd for $C_{48}H_{68}N_8O_{11}SNa^+$[M+Na]$^+$ 987.46240, found 987.46314.

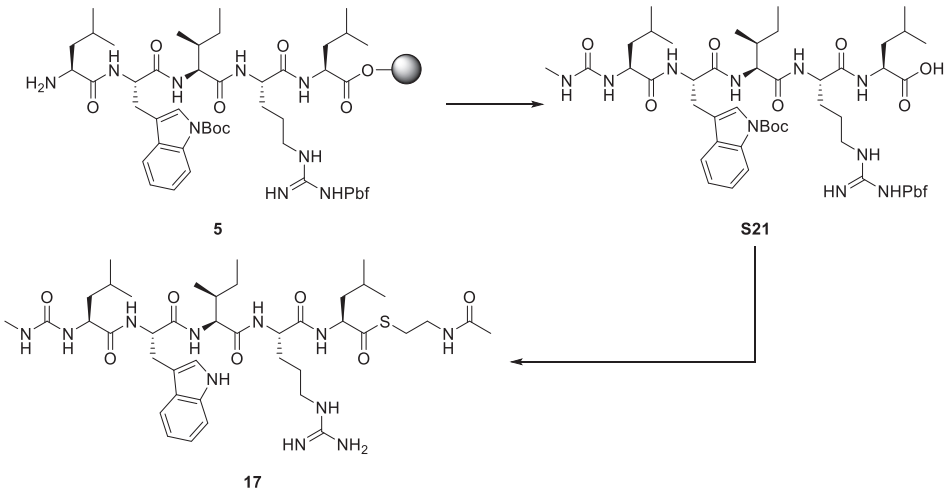

***seco*-bulbiferamide(F1Me)-SNAC (17)**: The resin **5** in Libra tube was swelled in CH_2Cl_2 for 10 min, and then the excess solvent was removed by filtration. To the resin was added a solution of *N*-succinimidyl methylcarbamate (69.8 mg, 0.40 mmol) in CH_2Cl_2 (0.5 mL), and shaken for 2 h at 40 °C. After the reaction mixture was filtered, washed with DMF (×3) and CH_2Cl_2 (×3), added HFIP/CH_2Cl_2 =3:7 (1.0 mL), shaken for 30 min, and filtered. This procedure was repeated 2 times to give ureido containing pentapeptide (**S21**). **S21** was used in the next reaction without further purification. To ureido containing pentapeptide **S21** in DMF (1 mL) were added PyBOP (104.2 mg, 0.20 mmol) and SNAC (22 μL, 0.20 mmol). After being stirred for 30 min at – 20 °C, added 2,6-lutidine (11 μL, 0.10 mmol) and stirred overnight at room temperature. The reaction mixtures were concentrated, and the peptides diluted with AcOEt and aqueous NH_4Cl. The resulting mixtures were extracted with AcOEt (×3), washed with brine, dried over Na_2SO_4 and concentrated. The residues were added TFA/phenol/*i*-Pr_3SiH/DODT =92.5:2.5:2.5:2.5 (3.0 mL). After Stirred for 2 h, the resulting mixtures were diluted with Et_2O (30 mL) and was chilled (–80 ℃), then centrifuged with 3,500 × *g* for 10 min at 4 ℃ to afford crude peptides. The crude peptides were purified by HPLC analytical condition 1 described in Table S5, to afford SNAC-substrate **17** (9.4 mg, 11.0% for 13 steps): ^{1}H NMR (500 MHz, DMSO-d_6): δ 10.76 (s, 1H), 8.50 (d, *J*= 7.5 Hz, 1H), 8.00 (m, 4H), 7.65 (d, *J*= 8.5 Hz, 1H), 7.48 (d, *J*= 8.0 Hz, 1H), 7.57-6.74 (m, 4H), 7.07 (s, 1H), 7.01 (t, *J*= 7.5 Hz, 1H), 6.91 (t, *J*= 8.0 Hz, 1H), 6.32 (br, 1H), 5.85 (br, 1H), 4.52-2.06 (m, 16H), 1.80-0.94 (m, 15H), 0.88-0.71 (m, 18H); ^{13}C NMR (125 MHz, DMSO-d_6): δ 201.9, 174.0, 172.2, 171.8, 171.2, 170.0, 158.9, 157.2, 136.5, 127.8, 123.9, 121.3, 118.8, 118.7, 111.8, 110.5, 58.0, 57.4, 53.8, 52.6, 52.5, 45.3, 45.3, 42.1, 38.6, 37.3, 36.9, 28.2, 27.3, 26.7, 25.6, 24.7, 24.6, 24.5, 23.6, 23.5, 23.0, 22.2, 21.4, 15.6, 11.6; HRMS (ESI) calcd for $C_{41}H_{68}N_{11}O_7S^+$[M+H]$^+$ 858.50076, found 858.50294.

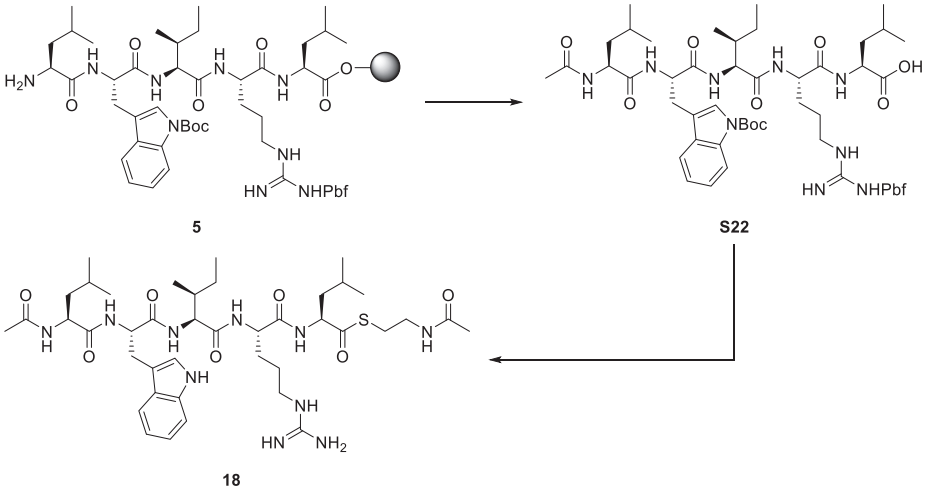

***seco*-*N*-Acetyl bulbiferamide-SNAC (18)**: The resin **5** in Libra tube was swelled in DMF for 10 min, which was subjected to 1 cycle [AcOH] of SPPS protocol described above (p4, Step1-4). After the reaction mixture was filtered, washed with DMF (×3) and CH_2Cl_2 (×3), added HFIP/CH_2Cl_2 =3:7 (1.0 mL), shaken for 30 min, and filtered. This procedure was repeated 2 times to give ureido containing peptapeptides (**S22**). **S22** was used in the next reaction without further purification. To ureido containing peptapeptides **S22** in DMF (1 mL) were added PyBOP (104.2 mg, 0.20 mmol) and SNAC (22 μL, 0.20 mmol). After being stirred for 30 min at – 20 °C, added 2,6-lutidine (11 μL, 0.10 mmol) and stirred overnight at room temperature. The reaction mixtures were concentrated, and the peptides diluted with AcOEt and aqueous NH_4Cl. The resulting mixtures were extracted with AcOEt (×3), washed with brine, dried over Na_2SO_4 and concentrated. The residues were added TFA/phenol/*i*-Pr_3SiH/DODT =92.5:2.5:2.5:2.5 (3.0 mL). After Stirred for 2 h, the resulting mixtures were diluted with Et_2O (30 mL) and was chilled (–80 °C), then centrifuged with 3,500 × *g* for 10 min at 4 °C to afford crude peptides. The crude peptides were purified by HPLC analytical condition 1 described in Table S5, to afford SNAC-substrate **18** (3.1 mg, 3.7% for 13 steps): ^{1}H NMR (500 MHz, DMSO-d_6): δ 10.78 (s, 1H), 8.51 (d, *J*= 6.4 Hz, 1H), 8.09-7.81 (m, 4H), 7.94 (d, *J*= 6.4 Hz, 1H), 7.65 (d, *J*= 6.8 Hz, 1H), 7.57-6.74 (br, 4H), 7.48 (d, *J*= 6.4 Hz, 1H), 7.06 (s, 1H), 7.01 (t, *J*= 6.0 Hz, 1H), 6.92 (t, *J*= 6.0 Hz, 1H), 4.53-4.47 (m, 1H), 4.38-4.29 (m, 2H), 4.25-4.15 (m, 2H), 3.62-2.30 (m, 8H), 1.80-0.94 (m, 18H), 0.88-0.71 (m, 18H); ^{13}C NMR (125 MHz, DMSO-d_6): δ 201.9, 172.8, 172.2, 171.7, 171.2, 170.0, 169.8, 157.2, 136.5, 129.8, 127.8, 121.3, 118.7, 111.7, 110.5, 110.1, 58.0, 57.2, 53.7, 52.5, 51.5, 49.1, 41.2, 40.9, 40.9, 38.6, 37.5, 29.4, 28.2, 27.4, 25.6, 24.6, 24.5, 23.5, 23.5, 23.0, 22.9, 22.1, 21.4, 15.6, 11.6; HRMS (ESI) calcd for $C_{41}H_{67}N_{10}O_7S^+[M+H]^+$ 843.48959, found 843.49204.

In silico analysis

Construction of an initial structure for MD simulation

Docking calculations were carried out using the Auto-Dock Vina [4]. The structure of BulbE TE predicted by AlphaFold2 was used for docking of bulbiferamide [1]. The conformation of bulbiferamide was previously described [5]. Polar hydrogens were included in the models. The search area included the entire active site cavity. The docking pose in which the cyclization point of bulbiferamide is close to the catalytic Cys731 was obtained for later manipulation (Figure S9a).

The structure of acyl-enzyme complex was manually modeled based on the docking pose under the following assumptions. First, the *C*-terminal Leu6 of the linear substrate forms a thioester bond with the catalytic Cys731 residue. Second, the experimental result indicated that the ureide structure is essential for macrocyclization. Third, the conformation of the bulbiferamide reflects the conformation of the tethered peptide. Considering these conditions, we obtained the initial structure of acyl-enzyme complex for MD simulation (Figure S9b).

MD simulation

The Amber ff14SB force field and the generalized Amber force field (GAFF) parameters were used for canonical amino acids and the ureide structure, respectively. The protein was protonated by the pdb4amber program in AmberTools [6]. The protein and ligand structures were solvated with the TIP3P water in a cubic box ($94 \times 70 \times 96$ $Å^3$) under periodic boundary conditions. Na^+ or Cl^- ions were included to neutralize the protein charge, then further ions were added corresponding to a salt solution of concentration 0.15 M. Protocols of energy minimization and equilibration of the system were previously described [7]. After the equilibration, a production run was performed in the NPT ensemble at 300 K for 20 ns. Coordinates were saved every 10 ps. These MD simulations were performed using GROMACS 2023 package [8].

TableS1. Oligonucleotides used in this study

Oligonucleotide	Sequence	Description	Reference
BulbE-TE_C731S_Fw	GGTGGATACTCTGAAGGTGCT	For BulbE-TE(C731S)	this study
BulbE-TE_C731S_Rv	AGCACCTTCAGAGTATCCACC	For BulbE-TE(C731S)	this study
BulbE-TE_E732Q_Fw	GGTGGATACTGTCAAGGTGCTATGG	For BulbE-TE(E732Q)	this study
BulbE-TE_E732Q_Rv	CCATAGCACCTTGACAGTATCCACC	For BulbE-TE(E732Q)	this study
BulbE-TE_T822I_Fw	ATGAGGCAATCCCAACTCA	For BulbE-TE(T822I)	this study
BulbE-TE_T822I_Rv	TGAGTTGGGATTGCCTCAT	For BulbE-TE(T822I)	this study
BulbE-TE_T824L_Fw	CAACCCCACTGCAAACGCT	For BulbE-TE(T824L)	this study
BulbE-TE_T824L_Rv	AGCGTTTGCAGTGGGGTTG	For BulbE-TE(T824L)	this study

TableS2. Plasmid used in this study

Plasmid	Description	Reference
BulbE-TE-pET28a	Expression plasmid of BulbE-TE	This study
BulbE-TE(C731S)-pET28a	Expression plasmid of BulbE-TE(C731S)	This study
BulbE-TE(E732Q)-pET28a	Expression plasmid of BulbE-TE(E732Q)	This study
BulbE-TE(T822I)-pET28a	Expression plasmid of BulbE-TE(T822I)	This study
BulbE-TE(T824L)-pET28a	Expression plasmid of BulbE-TE(T824L)	This study

TableS3. Strain used in this study

Strain	Description	Reference
E. coli DH5α	General host for gene cloning	Invitrogen
E. coli BL21 (DE3)	General host for protein expression	Novagen
E. coli BL21 (DE3)::BulbE-TE-pET28a	Expression host for BulbE-TE	This study
E. coli BL21 (DE3)::BulbE-TE(C731S)-pET28a	Expression host for BulbE-TE(C731S)	This study
E. coli BL21 (DE3)::BulbE-TE(E732Q)-pET28a	Expression host for BulbE-TE(E732Q)	This study
E. coli BL21 (DE3)::BulbE-TE(T822I)-pET28a	Expression host for BulbE-TE(T822I)	This study
E. coli BL21 (DE3)::BulbE-TE(T824L)-pET28a	Expression host for BulbE-TE(T824L)	This study

TableS4. Amino acid sequence of recombinant proteins used in this study

Protein	ID and description	Amino acid sequence
N-His6 tagged BulbE-TE	Amino acid sequence are derived from BulbE-TE (GenBank: WHI53517.1). Sequence from the expression vector pET28a is underlined.	MGSSHHHHHHSSGLVPRGSHMERELCLIWEKLLGVETIGVLDN FFDLGGDSILLLKVYHHCSRSNIRVSPKLLNEQPTIRGLAEKIKS QSIPNFSSCTENEIVDFLKDYNEFRKFMTFNGDSNKTGLFLIPAA AGPETFIPLVEKLDIDRPVQLLENIQVYSGRQIRLNHLIDYYLAV IRKKQPGGPYFLGGYCEGAMVSLGIAQKLEALGEQVEMLFLID PVVITIEQTMIDTIKQDSRLLECGRFEAEMVDTFLFYAEYVKSL HPYGGPAIFFEGSSVSDEATPTQTLALINDYIDIQGVFKKGFSTP KNGFEDLLLNCDYISIKAKHERVMIEDETLNTIAMAINRKLSTG QQTYLAPEAQTTEM*
N-His6 tagged BulbE-TE(C731S)	C731S mutants of BulbE-TE. The mutated residue was colored in red. Sequence from the expression vector pET28a is underlined.	MGSSHHHHHHSSGLVPRGSHMERELCLIWEKLLGVETIGVLDN FFDLGGDSILLLKVYHHCSRSNIRVSPKLLNEQPTIRGLAEKIKS QSIPNFSSCTENEIVDFLKDYNEFRKFMTFNGDSNKTGLFLIPAA AGPETFIPLVEKLDIDRPVQLLENIQVYSGRQIRLNHLIDYYLAV IRKKQPGGPYFLGGY**S**EGAMVSLGIAQKLEALGEQVEMLFLID PVVITIEQTMIDTIKQDSRLLECGRFEAEMVDTFLFYAEYVKSL HPYGGPAIFFEGSSVSDEATPTQTLALINDYIDIQGVFKKGFSTP KNGFEDLLLNCDYISIKAKHERVMIEDETLNTIAMAINRKLSTG QQTYLAPEAQTTEM*
N-His6 tagged BulbE-TE(E732Q)	E732Q mutants of BulbE-TE. The mutated residue was colored in red. Sequence from the expression vector pET28a is underlined.	MGSSHHHHHHSSGLVPRGSHMERELCLIWEKLLGVETIGVLDN FFDLGGDSILLLKVYHHCSRSNIRVSPKLLNEQPTIRGLAEKIKS QSIPNFSSCTENEIVDFLKDYNEFRKFMTFNGDSNKTGLFLIPAA AGPETFIPLVEKLDIDRPVQLLENIQVYSGRQIRLNHLIDYYLAV IRKKQPGGPYFLGGYC**Q**GAMVSLGIAQKLEALGEQVEMLFLID PVVITIEQTMIDTIKQDSRLLECGRFEAEMVDTFLFYAEYVKSL HPYGGPAIFFEGSSVSDEATPTQTLALINDYIDIQGVFKKGFSTP KNGFEDLLLNCDYISIKAKHERVMIEDETLNTIAMAINRKLSTG QQTYLAPEAQTTEM*
N-His6 tagged BulbE-TE(T822I)	T822I mutants of BulbE-TE. The mutated residue was colored in red. Sequence from the expression vector pET28a is underlined.	MGSSHHHHHHSSGLVPRGSHMERELCLIWEKLLGVETIGVLDN FFDLGGDSILLLKVYHHCSRSNIRVSPKLLNEQPTIRGLAEKIKS QSIPNFSSCTENEIVDFLKDYNEFRKFMTFNGDSNKTGLFLIPAA AGPETFIPLVEKLDIDRPVQLLENIQVYSGRQIRLNHLIDYYLAV IRKKQPGGPYFLGGYCEGAMVSLGIAQKLEALGEQVEMLFLID PVVITIEQTMIDTIKQDSRLLECGRFEAEMVDTFLFYAEYVKSL HPYGGPAIFFEGSSVSDEA**I**PTQTLALINDYIDIQGVFKKGFSTPK NGFEDLLLNCDYISIKAKHERVMIEDETLNTIAMAINRKLSTGQ QTYLAPEAQTTEM*
N-His6 tagged BulbE-TE(T824L)	T824L mutants of BulbE-TE. The mutated residue was colored in red. Sequence from the expression vector pET28a is underlined.	MGSSHHHHHHSSGLVPRGSHMERELCLIWEKLLGVETIGVLDN FFDLGGDSILLLKVYHHCSRSNIRVSPKLLNEQPTIRGLAEKIKS QSIPNFSSCTENEIVDFLKDYNEFRKFMTFNGDSNKTGLFLIPAA AGPETFIPLVEKLDIDRPVQLLENIQVYSGRQIRLNHLIDYYLAV IRKKQPGGPYFLGGYCEGAMVSLGIAQKLEALGEQVEMLFLID PVVITIEQTMIDTIKQDSRLLECGRFEAEMVDTFLFYAEYVKSL HPYGGPAIFFEGSSVSDEATP**L**QTLALINDYIDIQGVFKKGFSTP KNGFEDLLLNCDYISIKAKHERVMIEDETLNTIAMAINRKLSTG QQTYLAPEAQTTEM*

TableS5. Analytical conditions in this study

Condition	Description
1	column: COSMOSIL 5C_{18}- MS-II 20 ID × 250 mm (nacalai tesque) mobile phase: 40% MeCN + 0.05% TFA flow rate: 9.0 ml/min detector: SHIMADZU SPD-M20A prominence DIODE ARRAY DETECTOR
2	column: COSMOSIL 5C_{18}-MS-II 4.6 ID × 250 mm (nacalai tesque) mobile phase: gradient of (A) H_2O + 0.05% TFA / (B) MeCN + 0.05% TFA, B30-50% in 40 min flow rate: 1.0 ml/min detector: SHIMADZU SPD-M20A prominence DIODE ARRAY DETECTOR
3	column: COSMOSIL 5C_{18}-MS-II 4.6 ID × 250 mm mobile phase: 30% MeCN + 0.05% TFA flow rate: 1.0 ml/min detector: SHIMADZU SPD-M20A prominence DIODE ARRAY DETECTOR
4	column: COSMOSIL 5C_{18}-MS-II 2.0 ID × 150 mm (nacalai tesque) mobile phase: gradient of (A) H_2O + 0.05% TFA / (B) MeCN + 0.05% TFA, B2-98% in 15 min flow rate: 0.2 ml/min detector: amaZon SL-NPC operated in positive mode, coupled with a SHIMADZU HPLC system

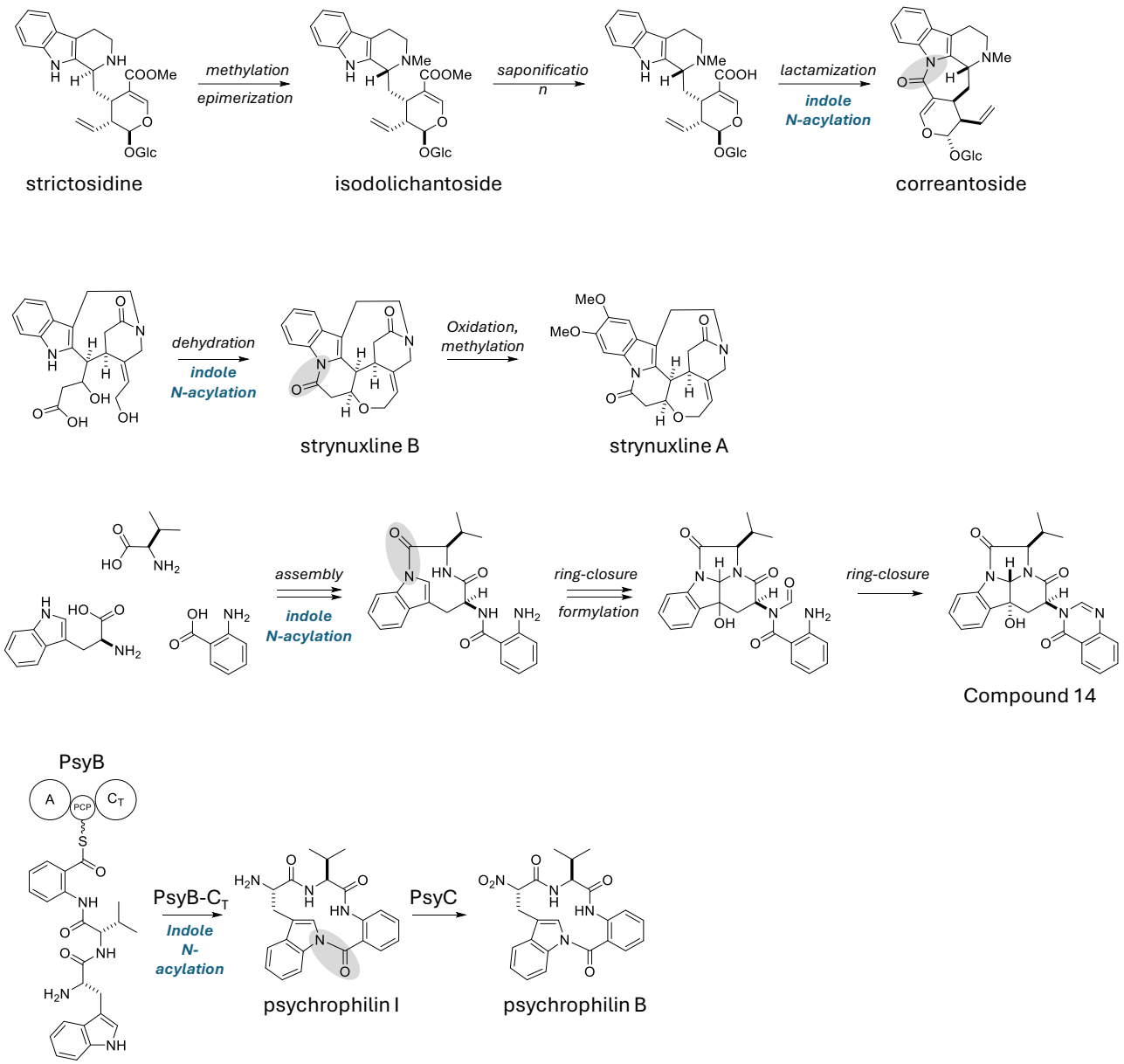

Figure S1. Hypothetical biosynthetic pathways of natural products which involve indole *N*-acylations. These include the biosynthesis of correantoside[9], strynuxline[10], compound 14[11], and psychrophilin[12]. Bonds formed via indole *N*-acylations are highlighted by shading.

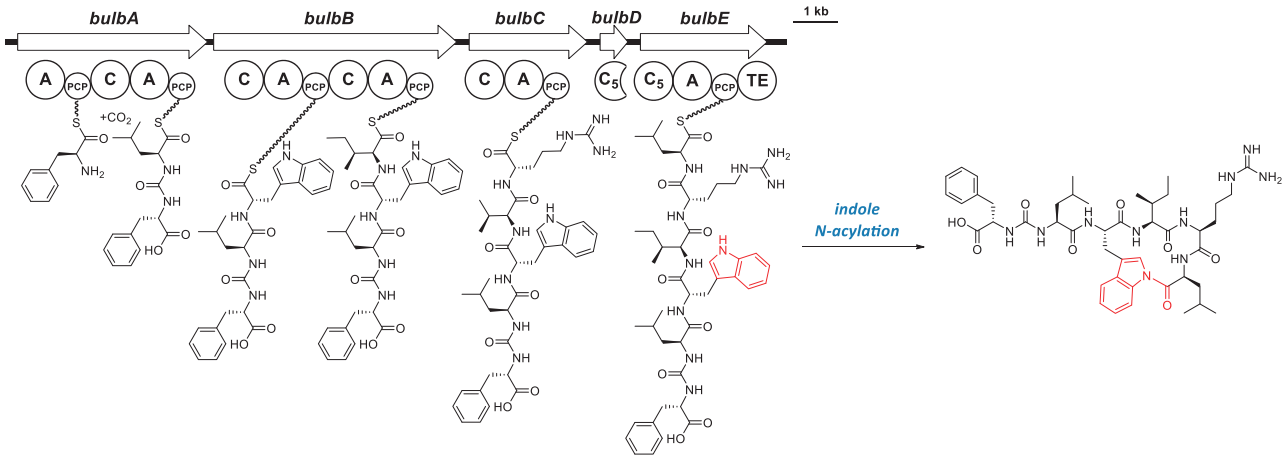

Figure S2. The proposed biosynthetic pathway of bulbiferamide[13]. This pathway predicted from the modular organization of the NRPS as follows. First, L-phenylalanine is loaded into BulbA and carbon dioxide is introduced into the amine [14], which then reacts with L-Leu to form ureido structure. Next, L-tryptophan, L-isoleucine, L-arginine, and L-leucine are elongated in turn by BulbB, C, D and E. Finally, a cyclic skeleton containing *N*-acylindole is formed.

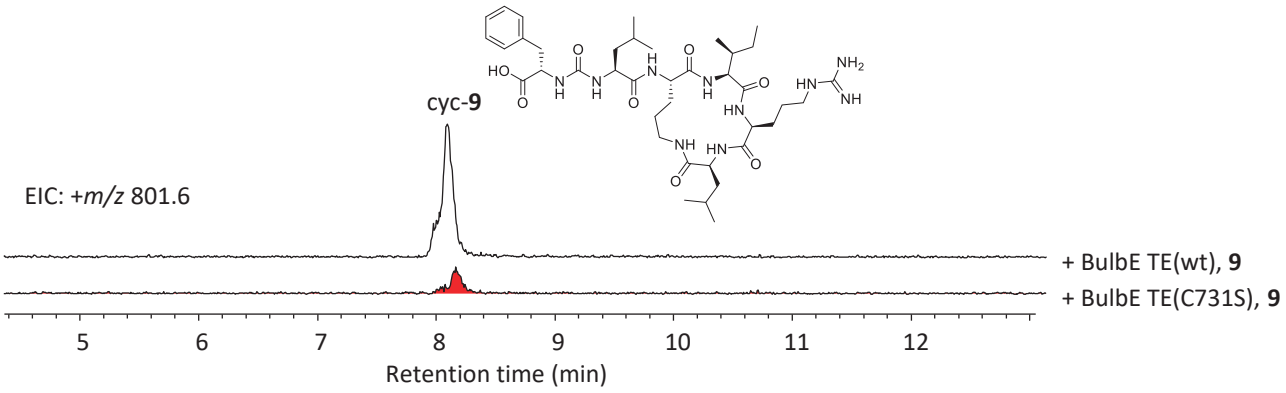

Figure S3. LC-MS analysis of BulbE TE reaction mixtures with **9** as a substrate (LCMS analytical condition 4 described in Table S5). Extracted ion chromatograms of *m/z* 801.6, which correspond to cyc-**9**, are shown. The peak of cyc-**9** generated by BulbE TE(C731S) is colored red.

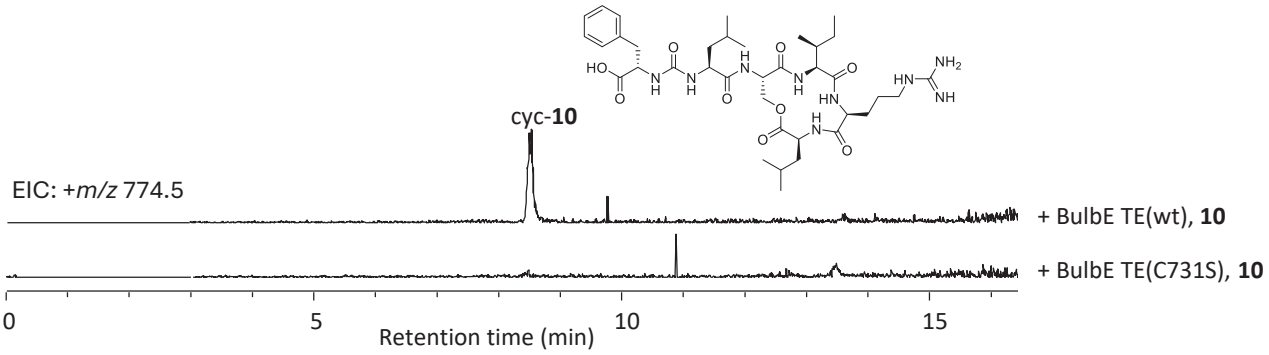

Figure S4. LC-MS analysis of BulbE TE reaction mixtures with **10** as a substrate (LCMS analytical condition 4 described in Table S5). Extracted ion chromatograms of *m/z* 774.5, which correspond to cyc-**10**, are shown.

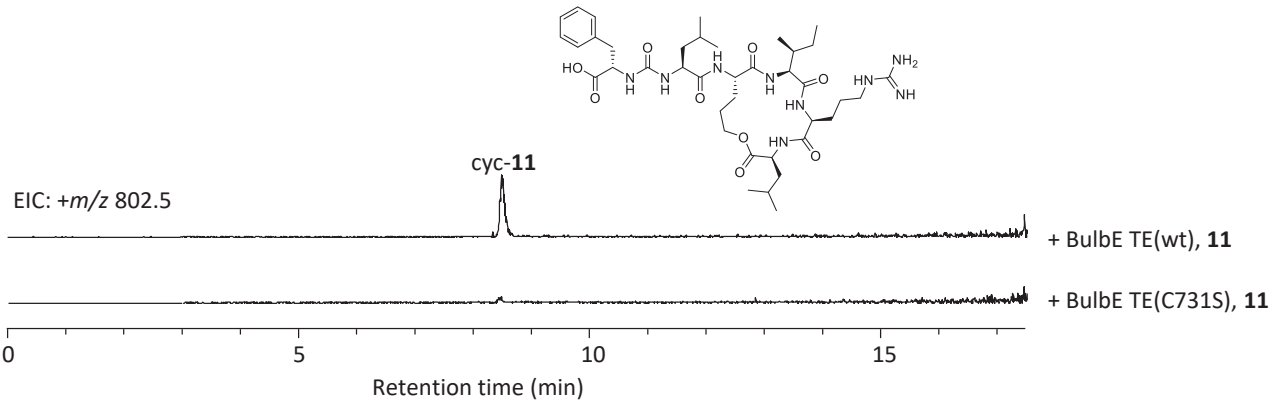

Figure S5. LC-MS analysis of BulbE TE reaction mixtures with **11** as a substrate (LCMS analytical condition 4 described in Table S5). Extracted ion chromatograms of *m/z* 802.5, which correspond to cyc-**11**, are shown.

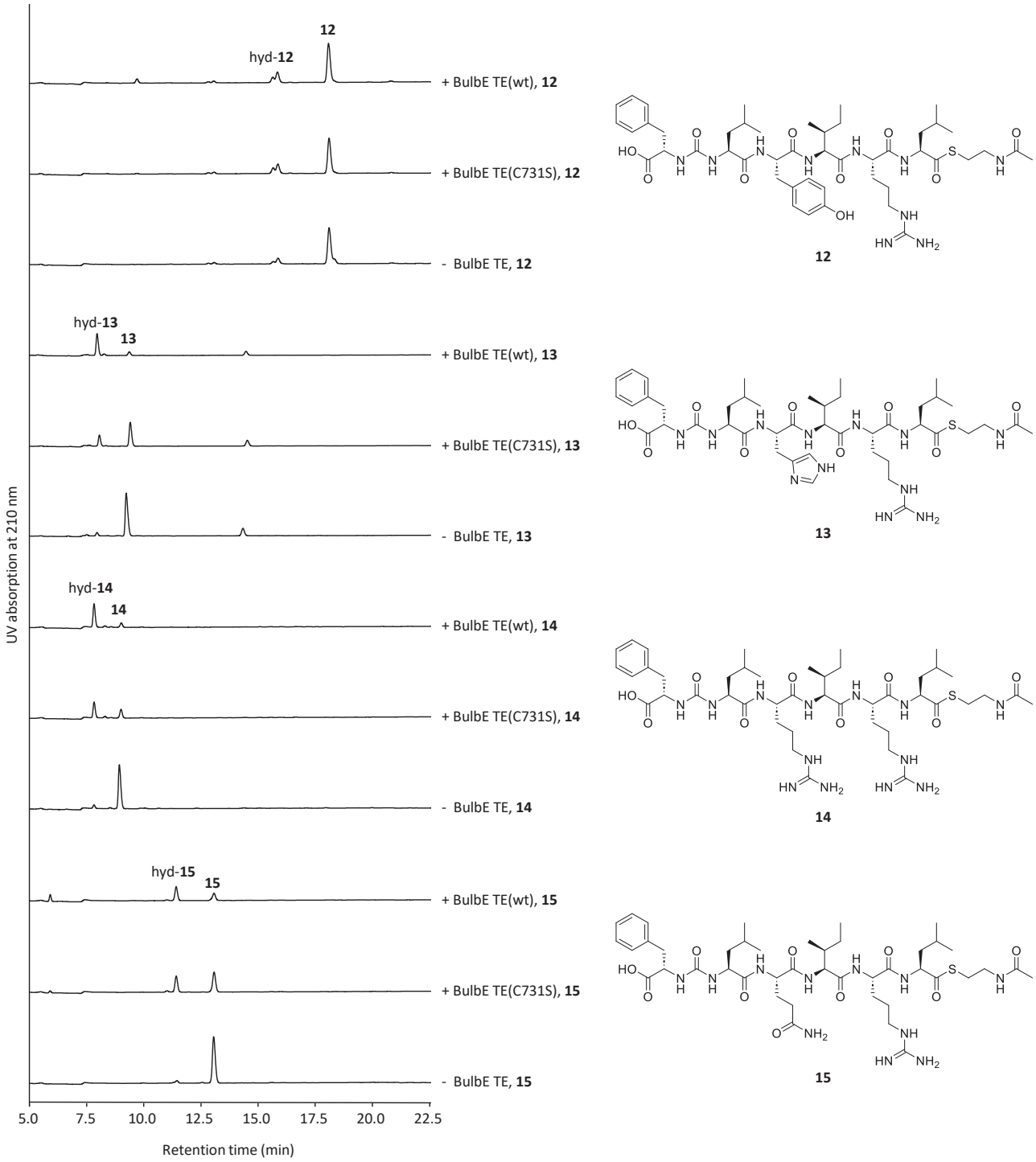

Figure S6. Analysis of BulbE TE reaction mixtures with **12-15** as a substrate. HPLC analytical condition 2 described in Table S5. The structures of substrate are depicted.

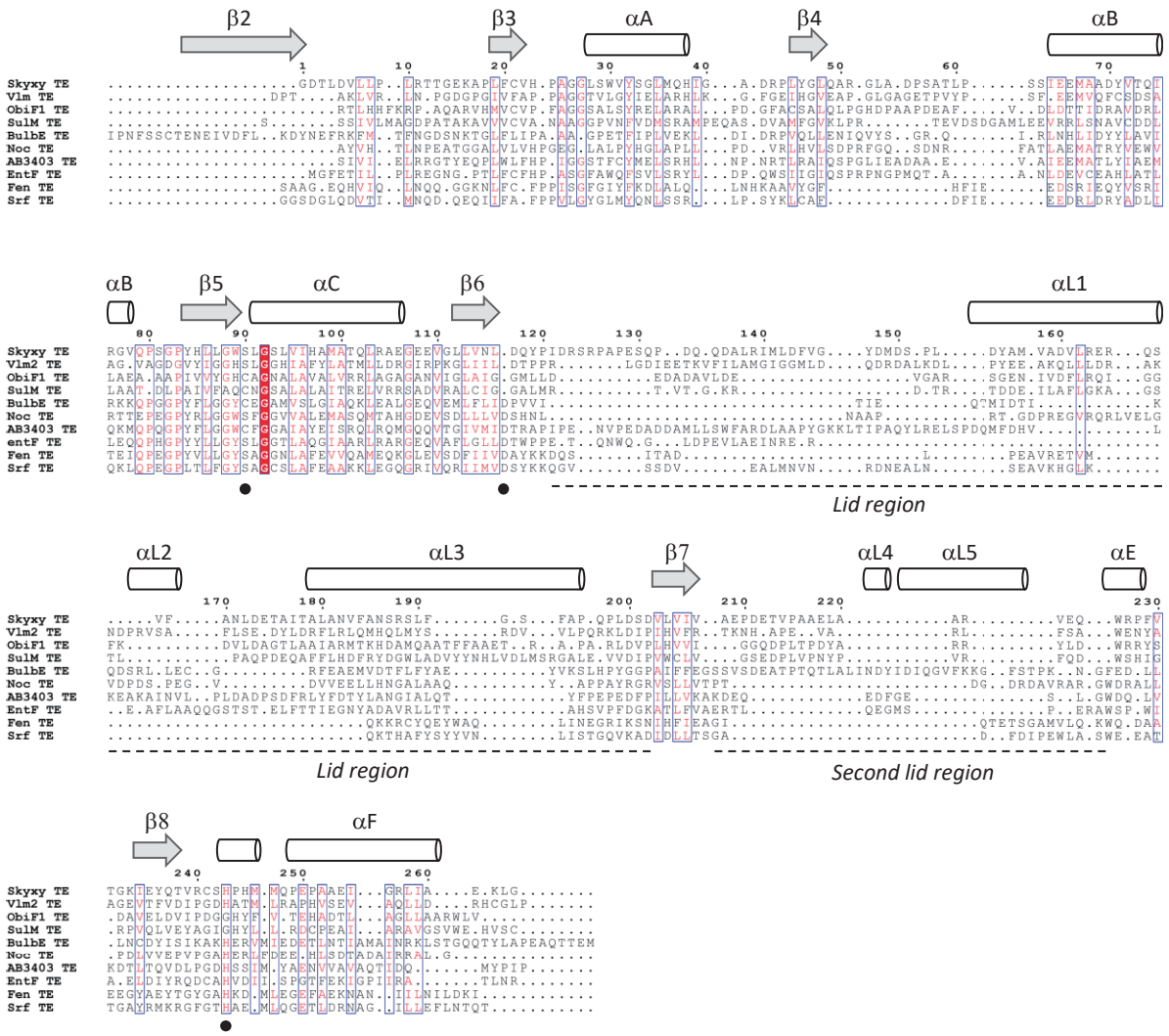

Figure S7. Multiple structure alignment of NRPS TEs. Secondary elements and lid regions were depicted above and below the alignment, respectively, in accordance with the BulbE TE Alphafold model. The catalytic triad (Cys731/His867/Asp758 in BulbE TE) are highlighted by black circles. The structures used for this alignment are SkyXY TE (7CRN), Vlm2 TE (6ECE), ObiF TE (6N8E), SulM TE (8W2C), BulbE TE (generated by AlphaFold2[1] in this study), Noc TE (6OJD), AB3403 TE (4ZXI), EntF (3TEJ), Fen TE (2CB9) and Srf TE (8W2C). Structures were aligned by FoldMason[15] with 1000 iteration of refinement. The figure was generated by EsPript3.0[16].

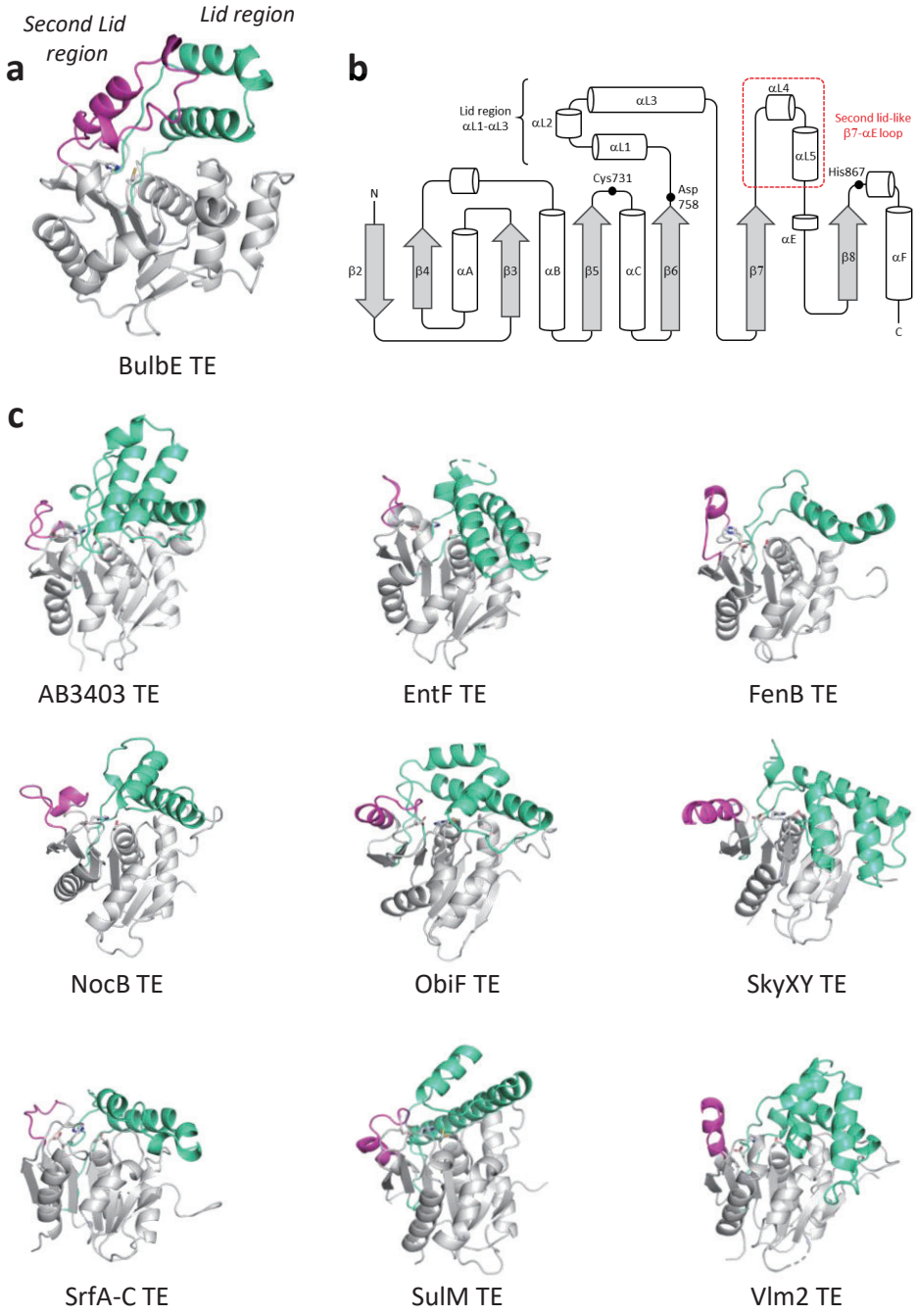

Figure S8. Comparison of the lid regions and second lid regions between different NRPS thioesterases. **a.** Alphafold 2 model of BulbE TE. The lid region (β6-β7) and second lid region (β7-αE) are colored in cyan and magenta, respectively. The core region with α/β hydrolase fold is colored gray. Side chains of catalytic triad are shown as sticks. **b.** Topology diagram of BulbE TE. The catalytic triad is depicted as black circles. The identical figure is shown in the main manuscript as Figure 3a. **c.** Structure of NRPS thioesterases. Color scheme is identical to the panel a. The lid regions (between β6-β7, cyan) and second lid region (between β7-αE, magenta) are highly varied among NRPS TEs. The second lid region of BulbE TE in panel a is uniquely long among NRPS TEs. PDB IDs of the structures are as follows: SkyXY TE (7CRN), Vlm2 TE (6ECE), ObiF TE (6N8E), SulM TE (8W2C), Noc TE (6OJD), AB3403 TE (4ZXI), EntF (3TEJ), Fen TE (2CB9) and Srf TE (8W2C).

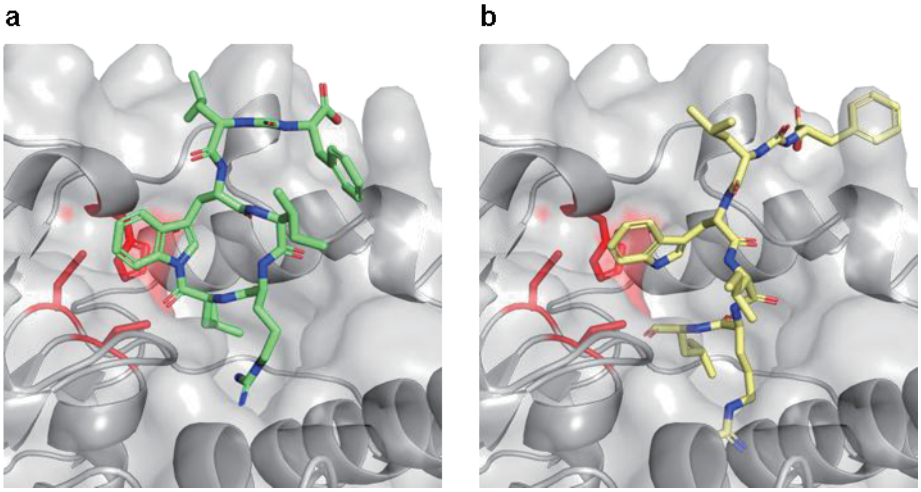

Figure S9. Comparison of the conformations of bulbiferamide.
The docking pose (a), the initial structure for MD simulation (b), and BulbE TE are shown in green, yellow, and gray, respectively. The catalytic triad is shown in red.

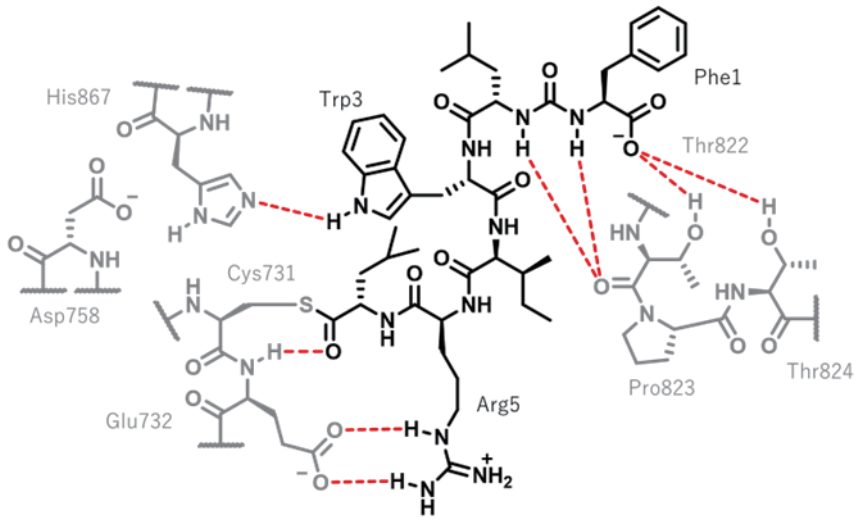

Figure S10. The overview of substrate recognition of BulbE TE
Polar interactions in acyl-enzyme complex model of BulbE TE are depicted as red dots.

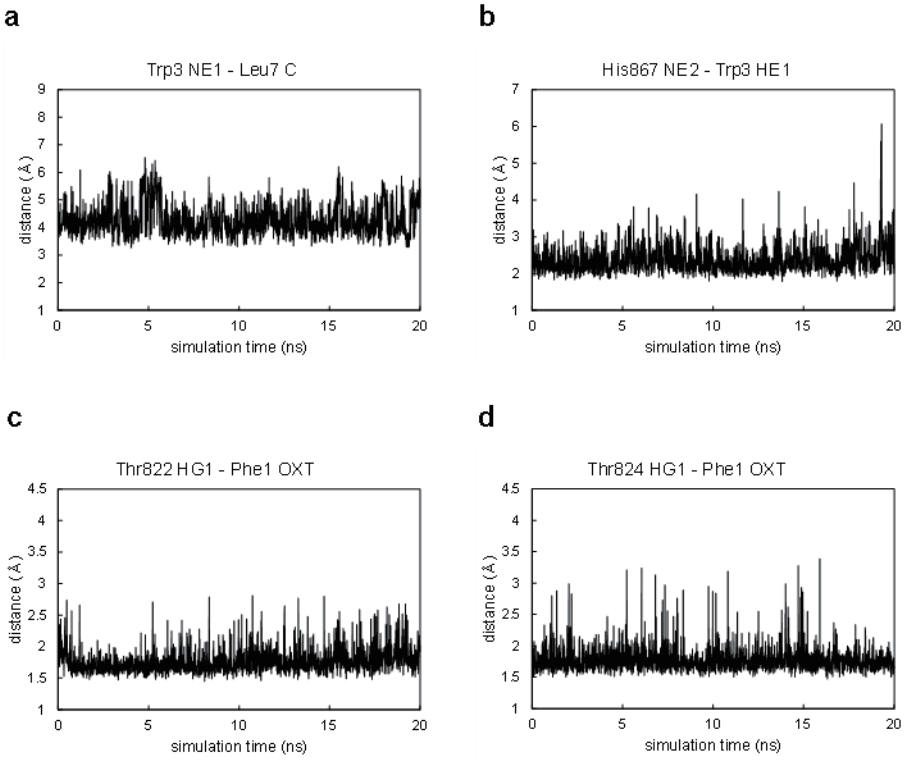

Figure S11. Plots of the interatomic distances in the 20 ns MD simulation.

a-d. Plots of the distances between the nucleophile indole nitrogen of Trp3 (Trp3 NE1) and the reactive thioester carbon of Leu6 (Leu6 C) (a), between the basic nitrogen of His867 (Hi867 NE2) and the indole hydrogen of Trp3 (Trp3 HE1) (b) , between β-OH of Thr822 (Thr822 HG1) and the carboxylate oxygen of the *pseudo*-*C*-terminus Phe1 (Phe1 OXT) (c) , and between β-OH of Thr824 (Thr824 HG1) and Phe1 OXT (d) in the 20 ns MD simulations. The average distances are 4.27 Å (a), 2.37 Å (b), 1.77 Å (c), and 1.78 Å (d), respectively.

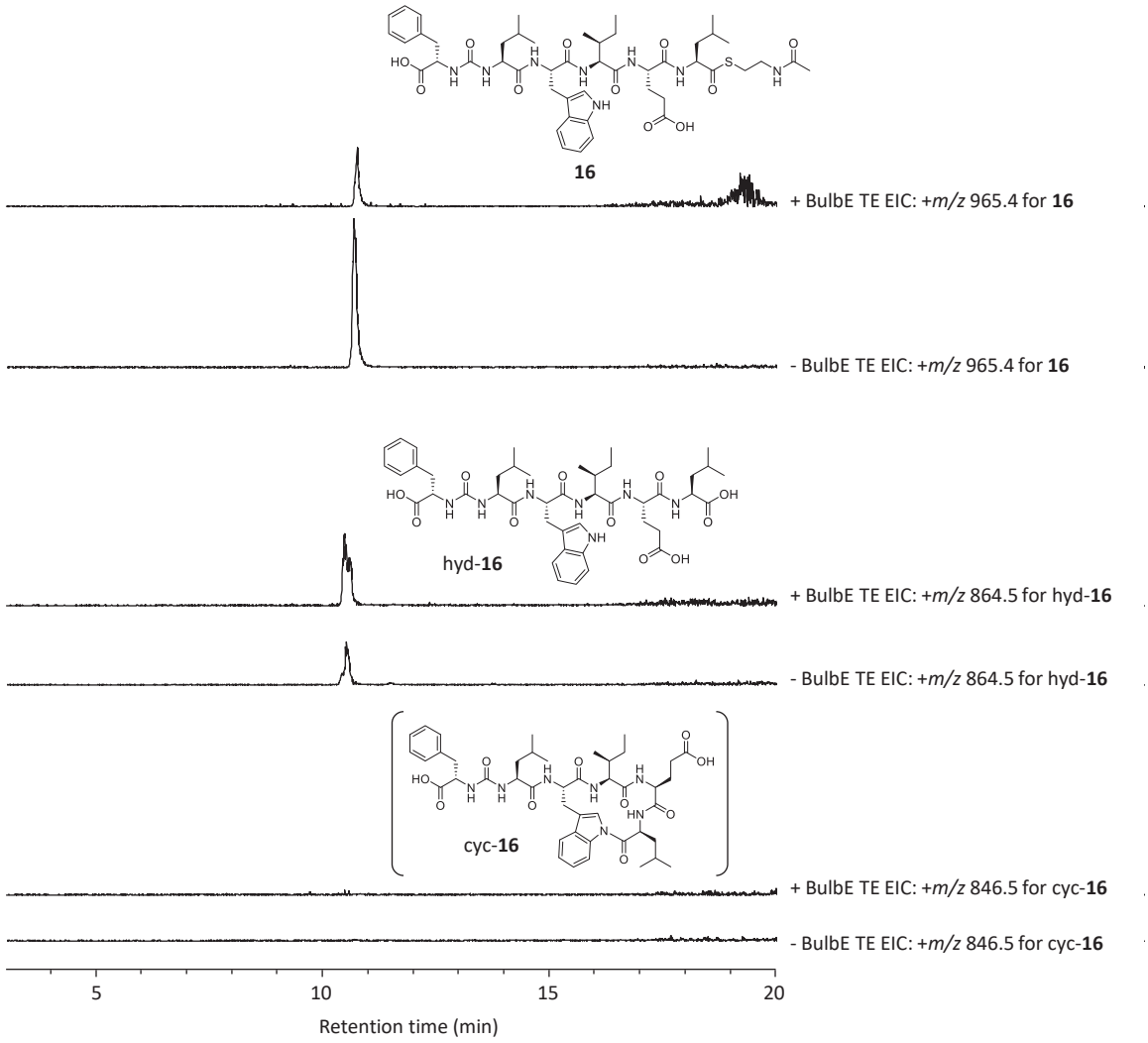

Figure S12. LC-MS analysis of BulbE TE reaction mixtures with **16** as a substrate (LCMS analytical condition 4 described in Table S5). EICs corresponding to **16** (*m/z* 965.4), hyd-**16** (*m/z* 864.5), cyc-**16** (*m/z* 846.5) are shown. Substrate **16** was consumed while hyd-**16** accumulated in an enzyme-dependent manner. Cyclized product (cyc-**16**) was not observed.

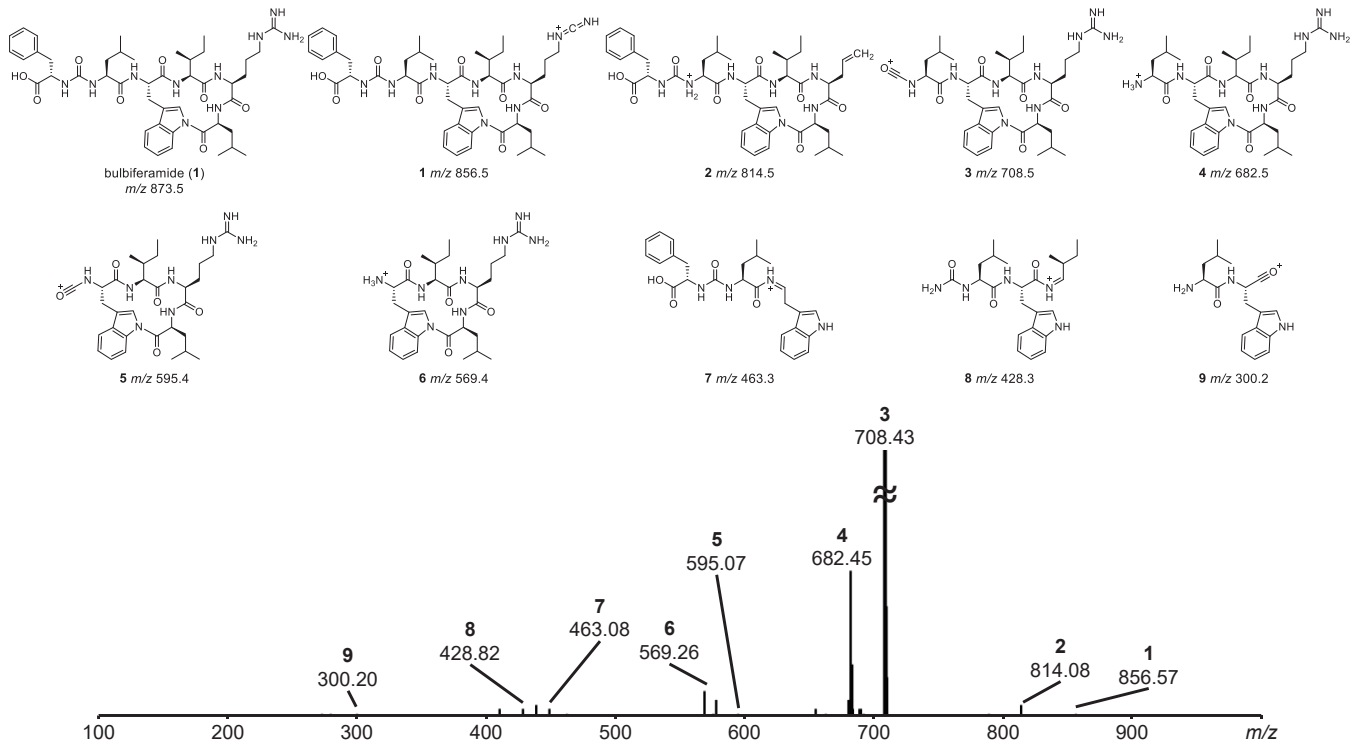

Figure S13. MS2 spectrum of bulbiferamide (**1**)

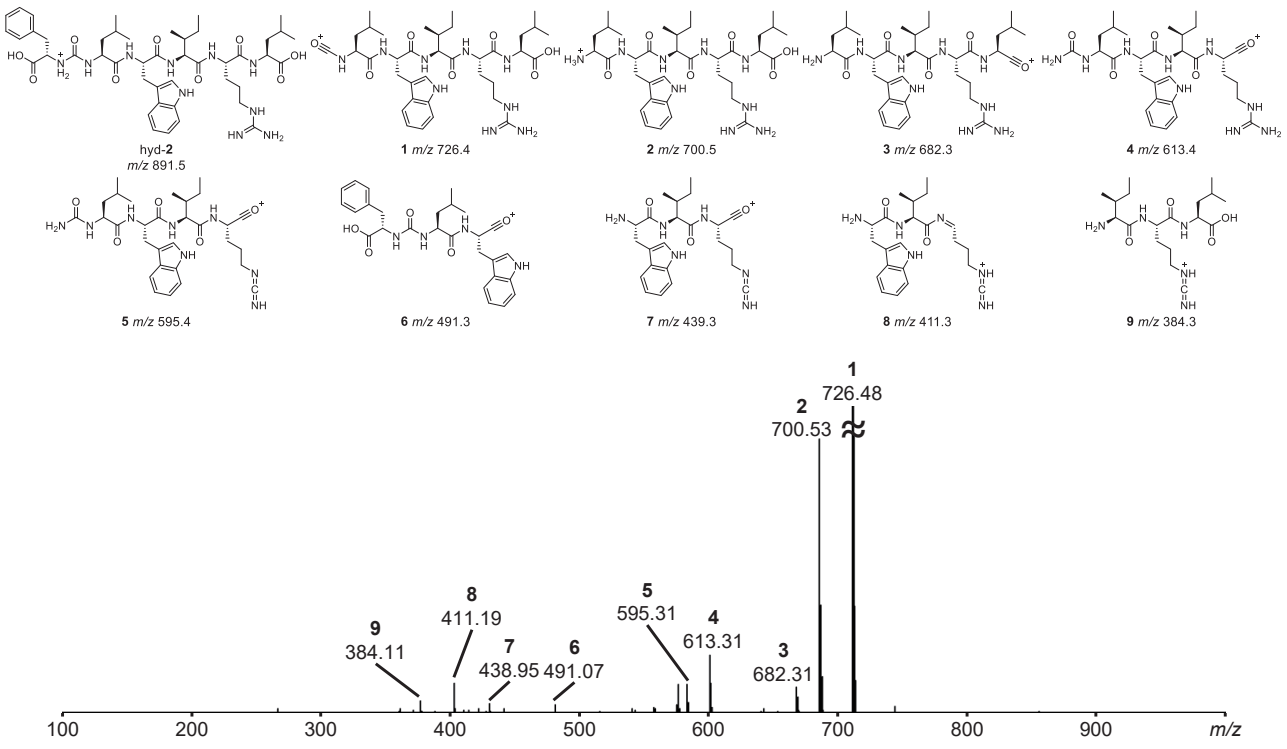

Figure S14. MS2 spectrum of *seco*-bulbiferamide (hyd-**2**)

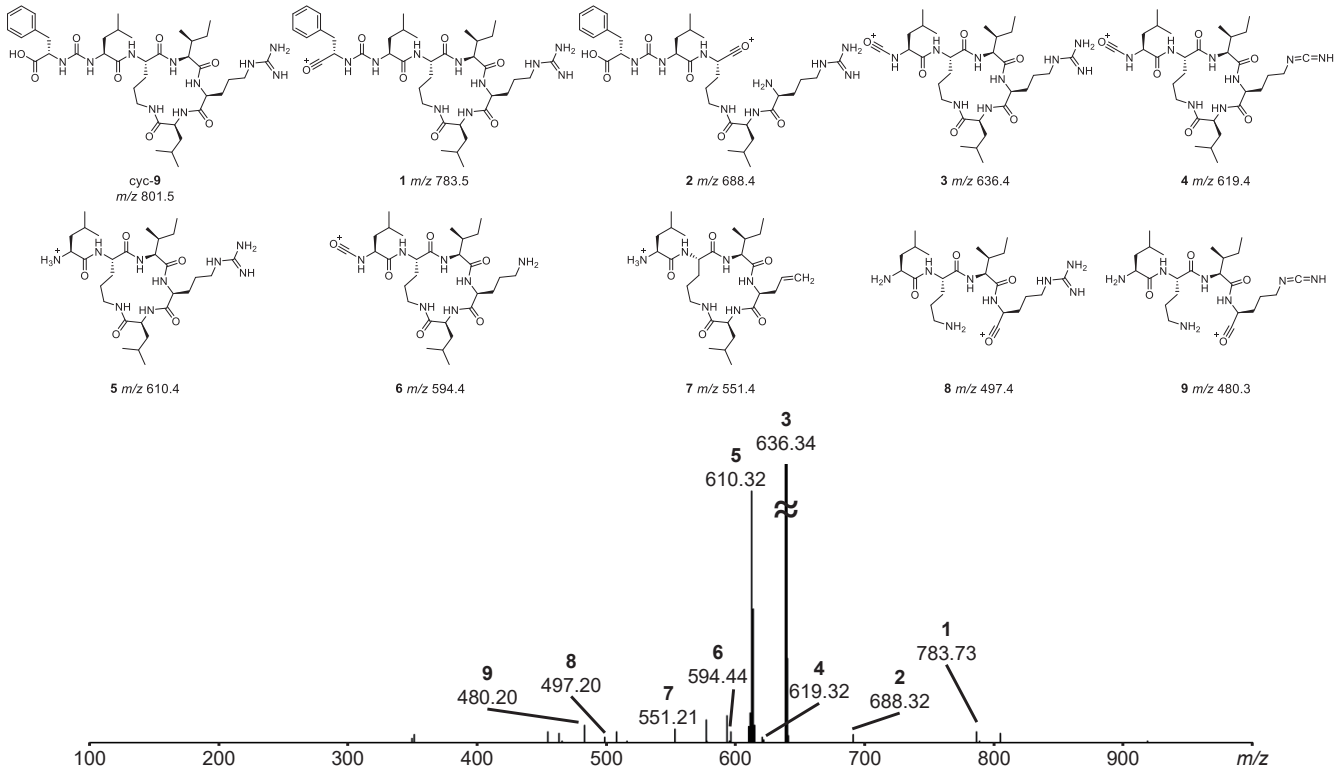

Figure S15. MS2 spectrum of cyc-**9**

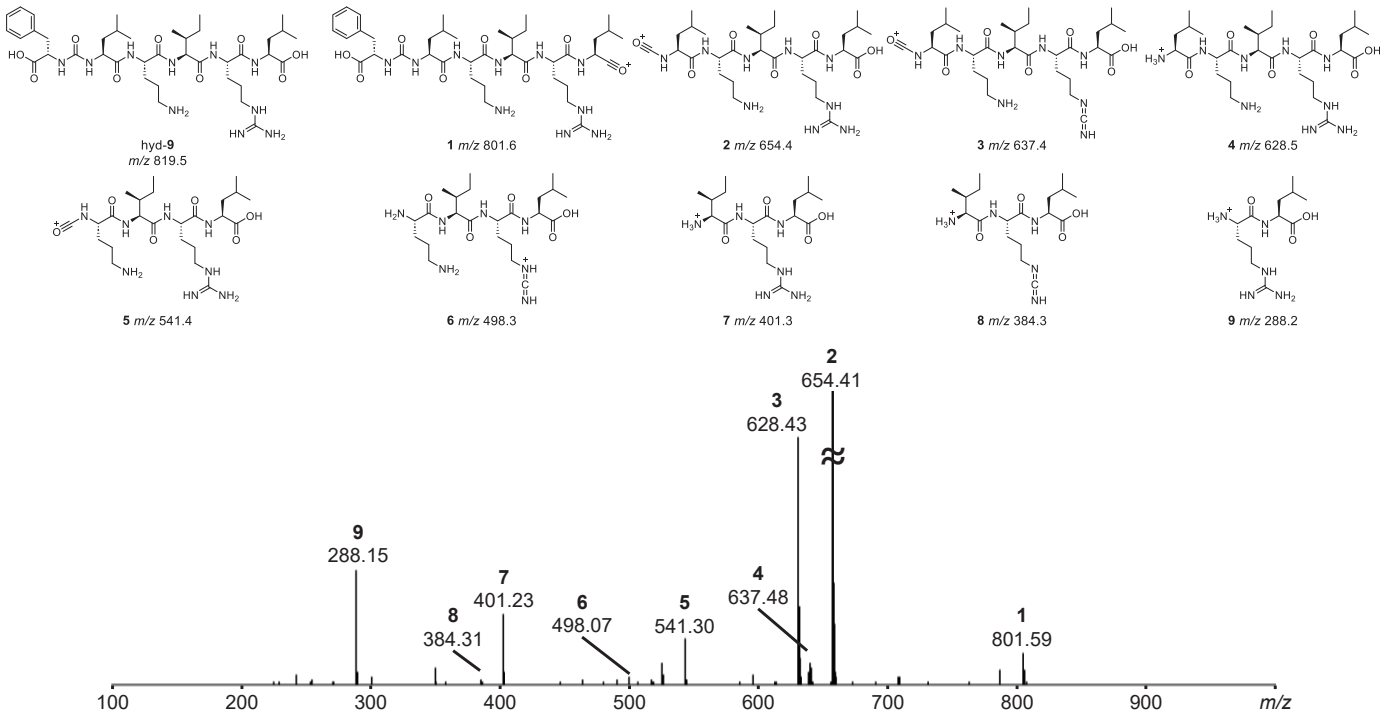

Figure S16. MS2 spectrum of hyd-**9**

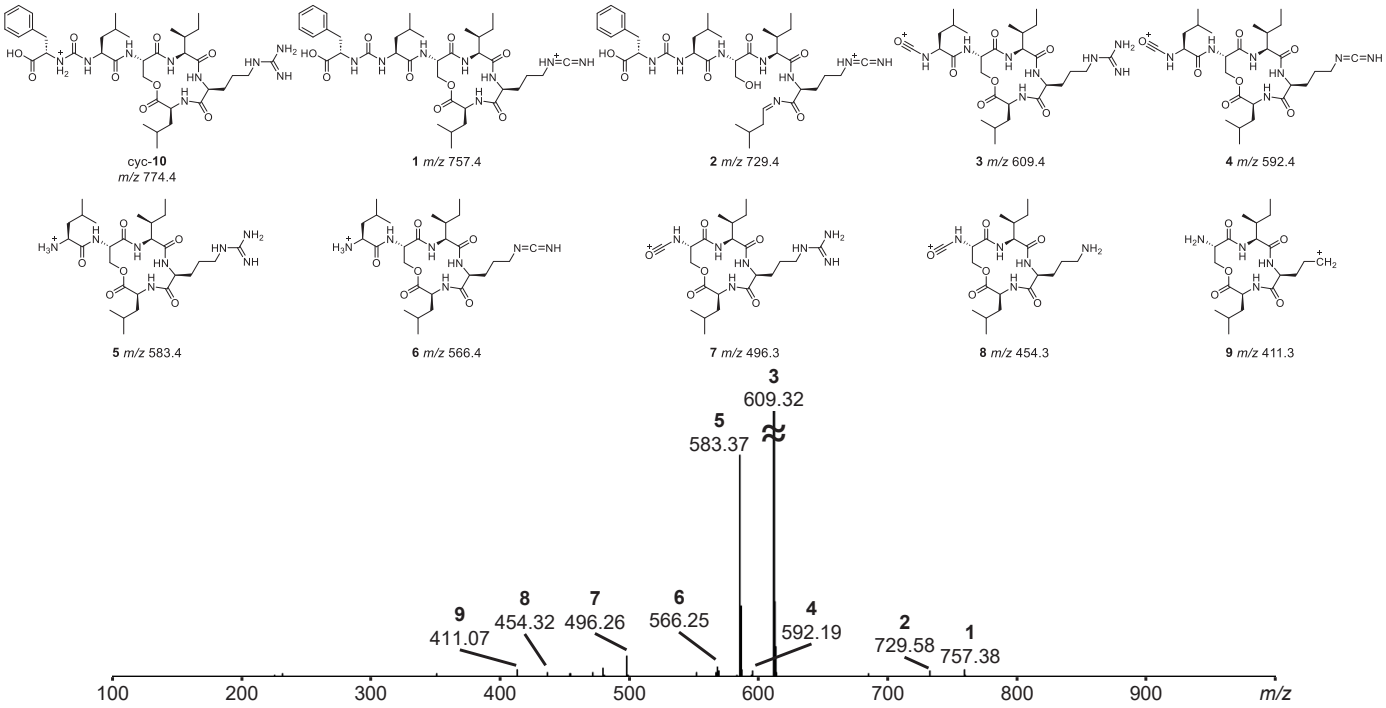

Figure S17. MS2 spectrum of cyc-**10**

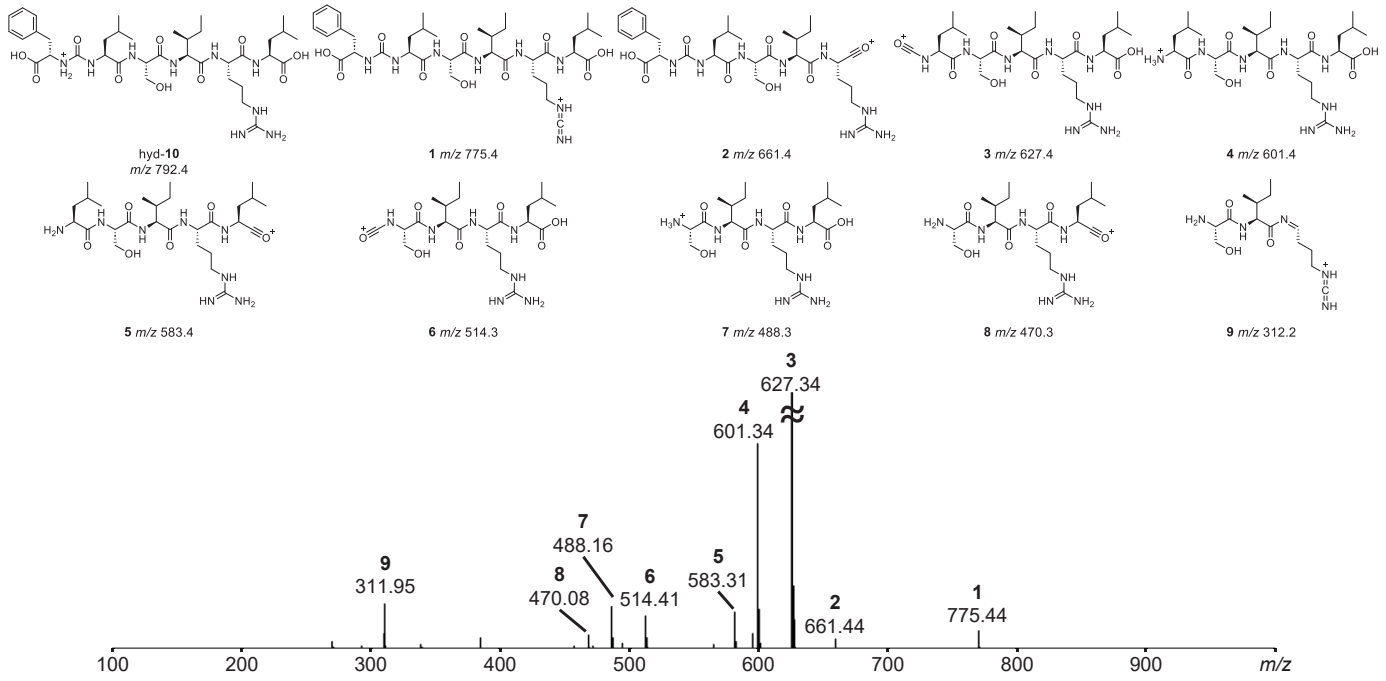

Figure S18. MS2 spectrum of hyd-**10**

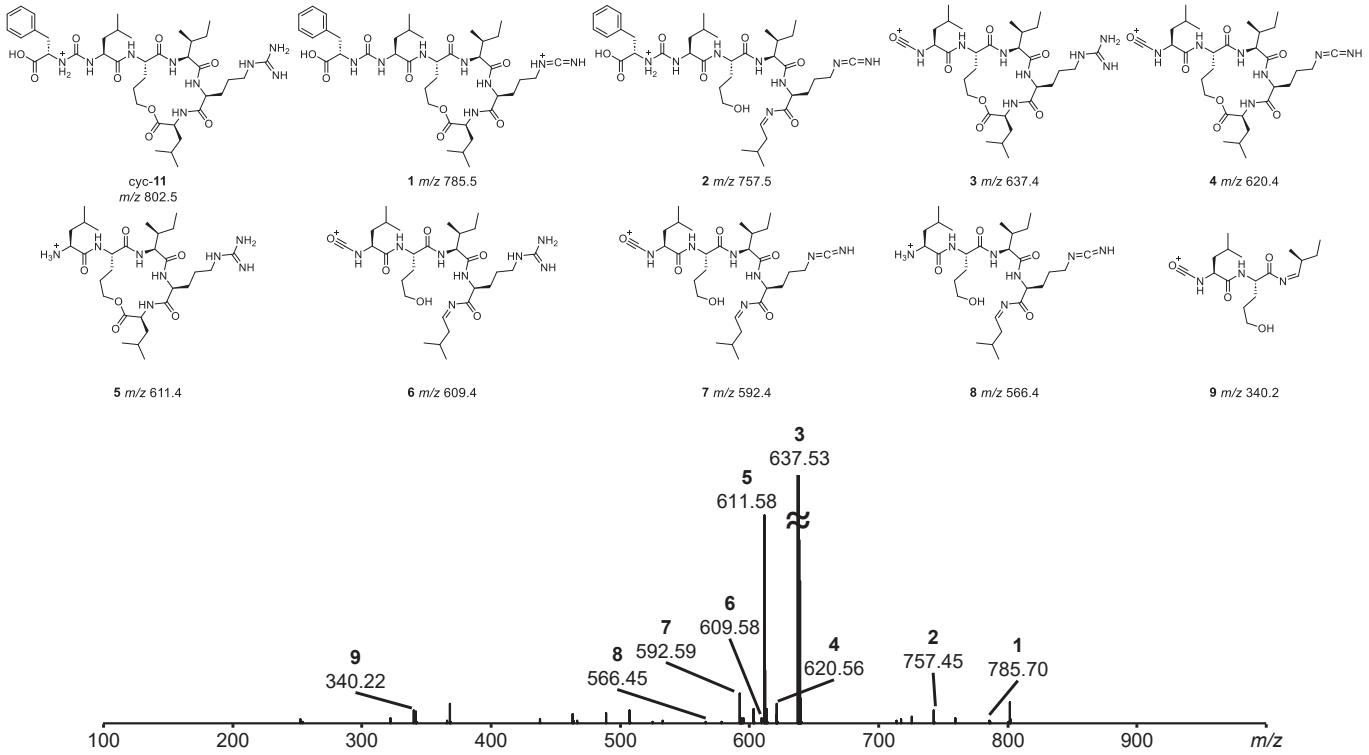

Figure S19. MS2 spectrum of cyc-**11**

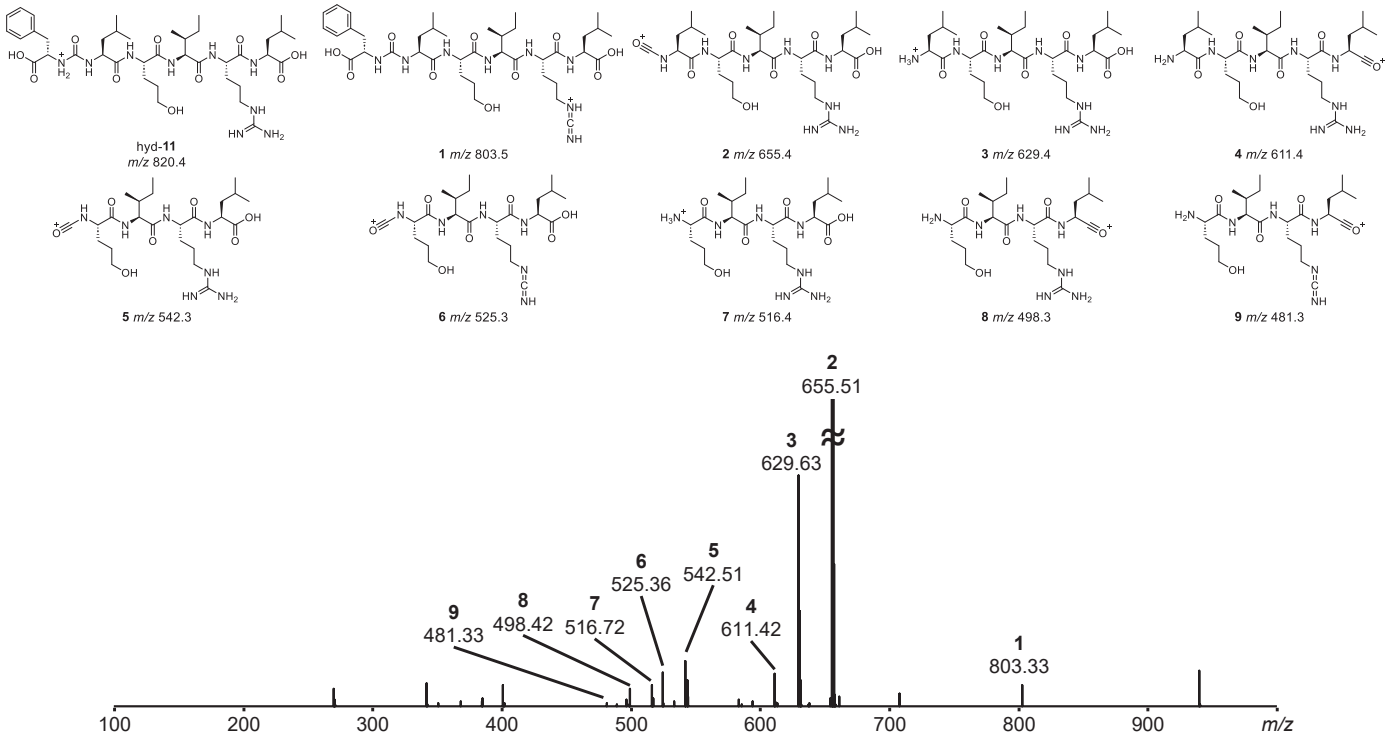

Figure S20. MS2 spectrum of hyd-**11**

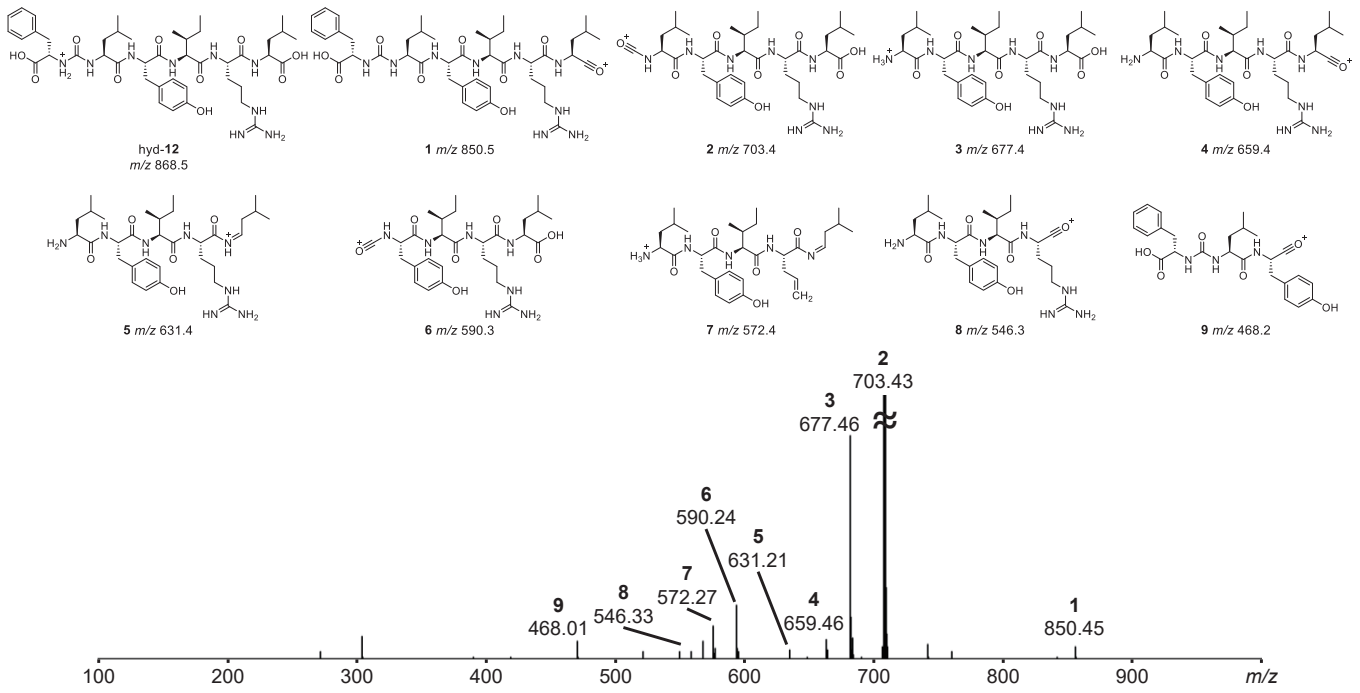

Figure S21. MS2 spectrum of hyd-**12**

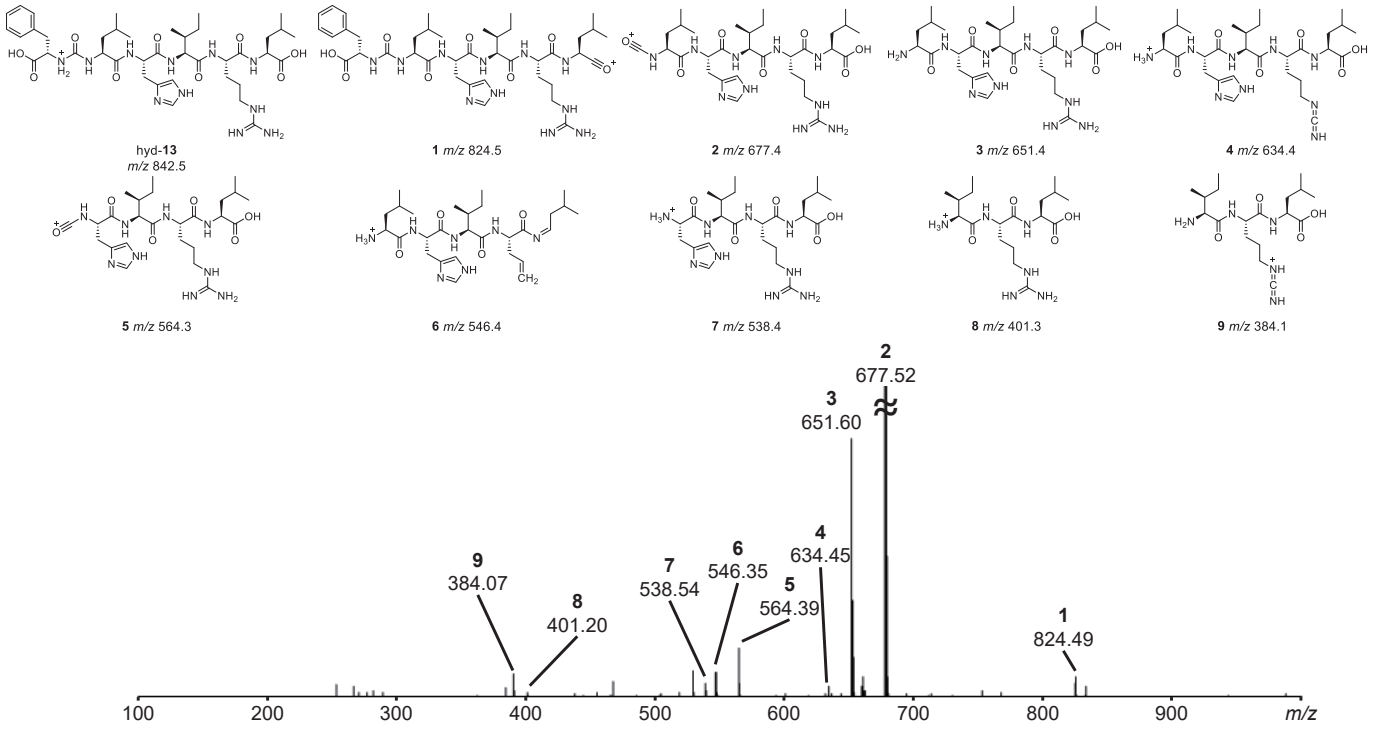

Figure S22. MS2 spectrum of hyd-**13**

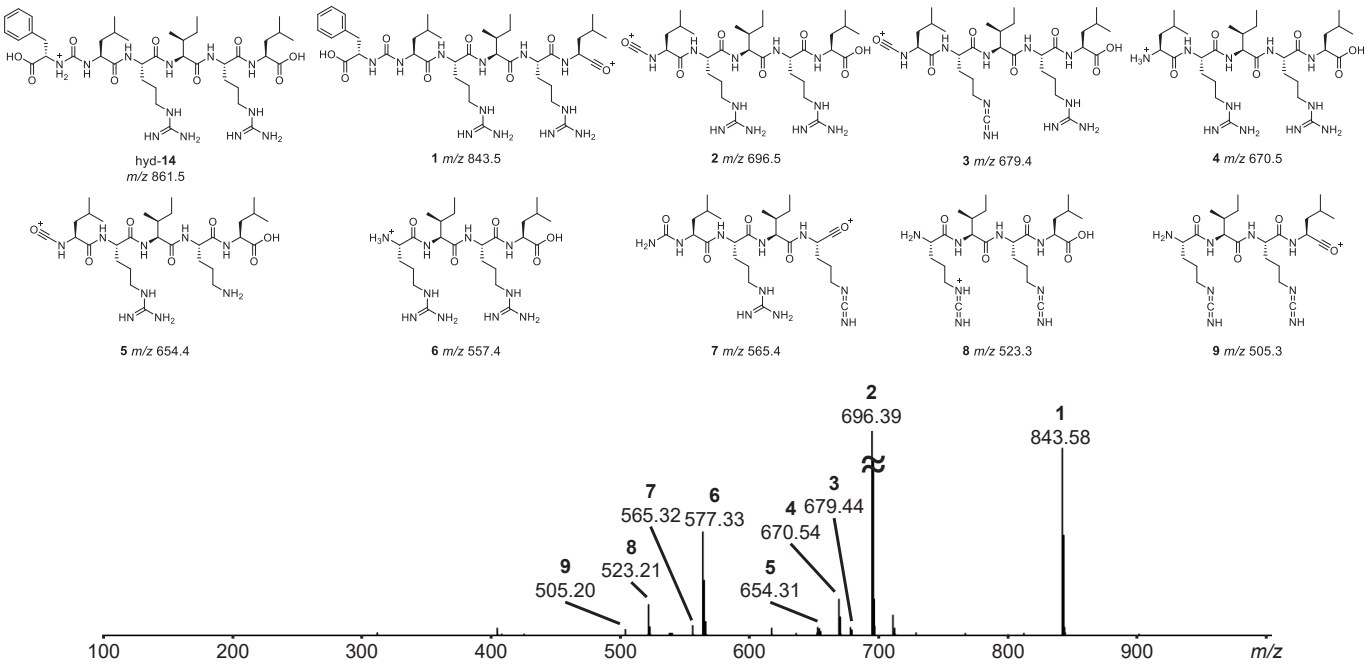

Figure S23. MS2 spectrum of hyd-**14**

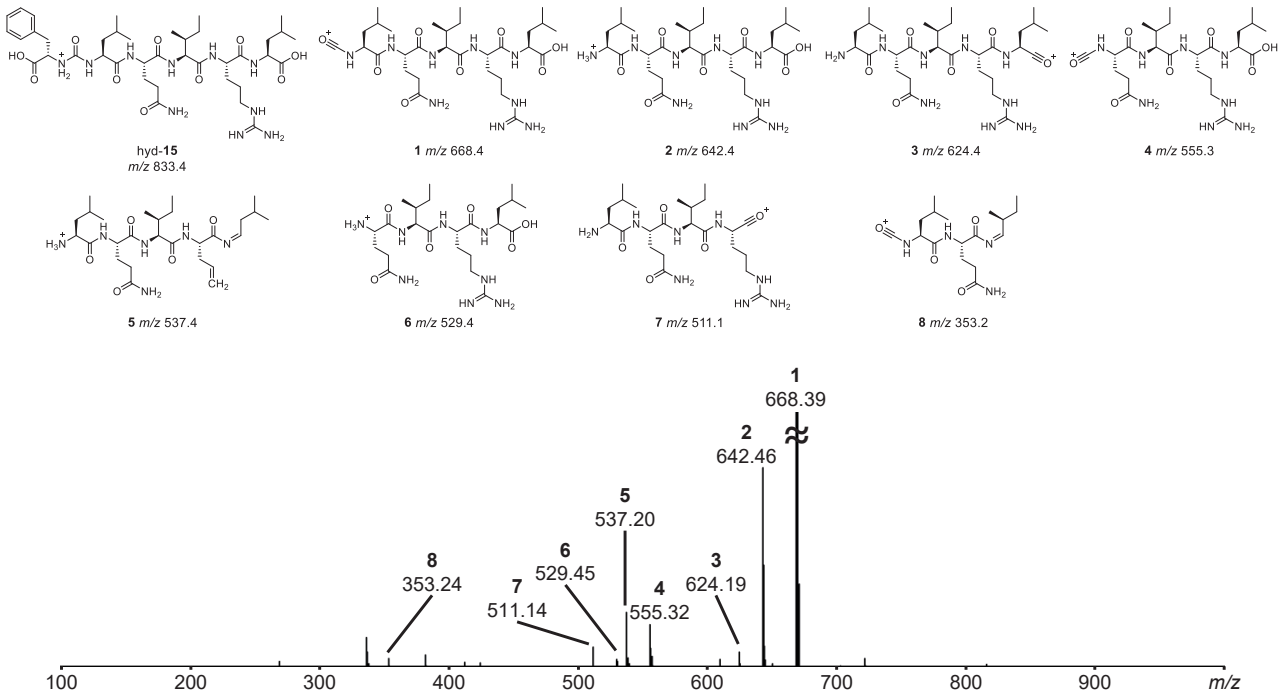

Figure S24. MS2 spectrum of hyd-**15**

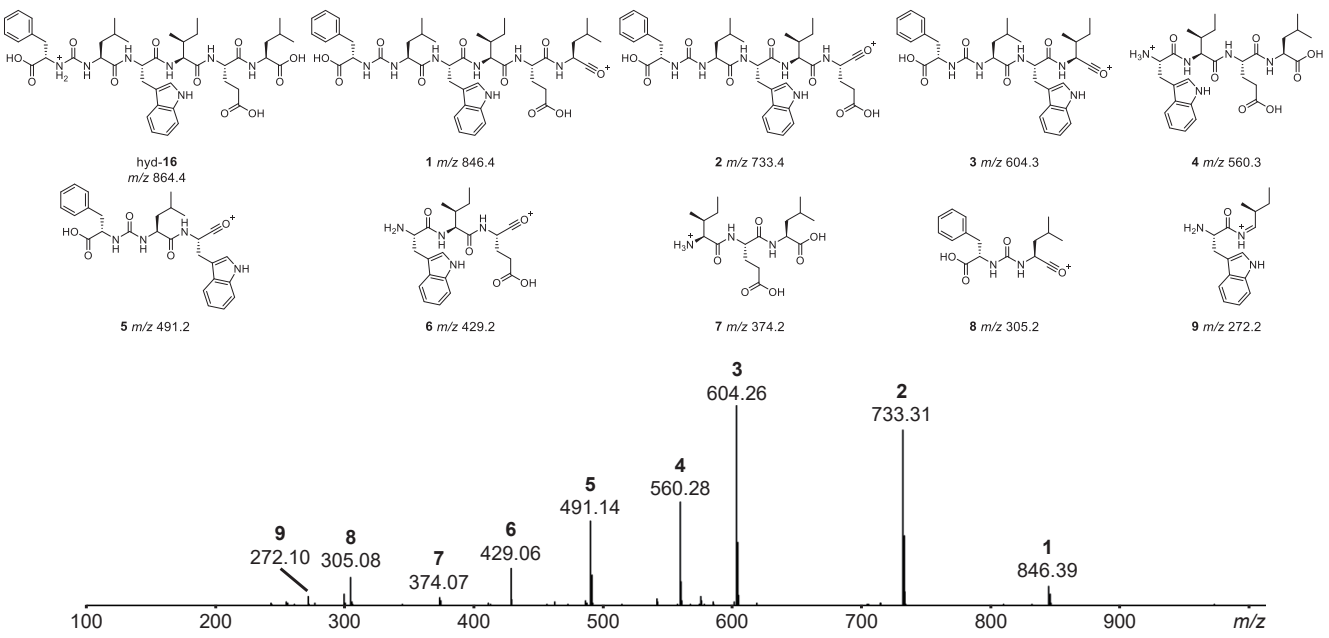

Figure S25. MS2 spectrum of hyd-**16**

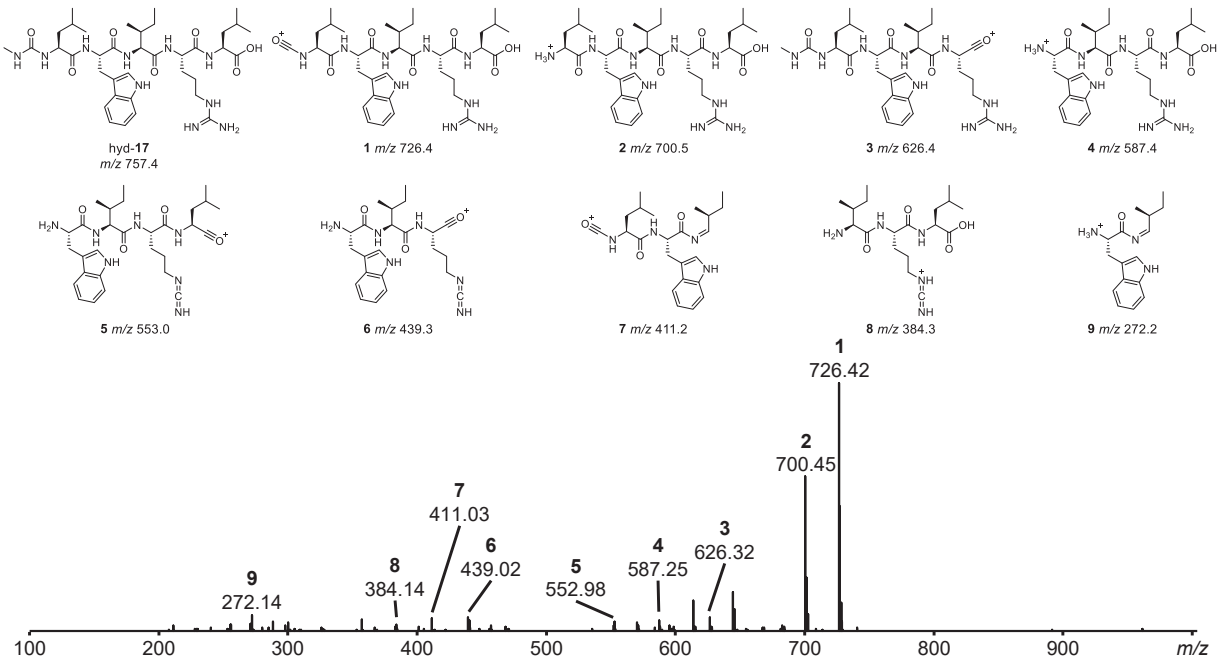

Figure S26. MS2 spectrum of hyd-**17**

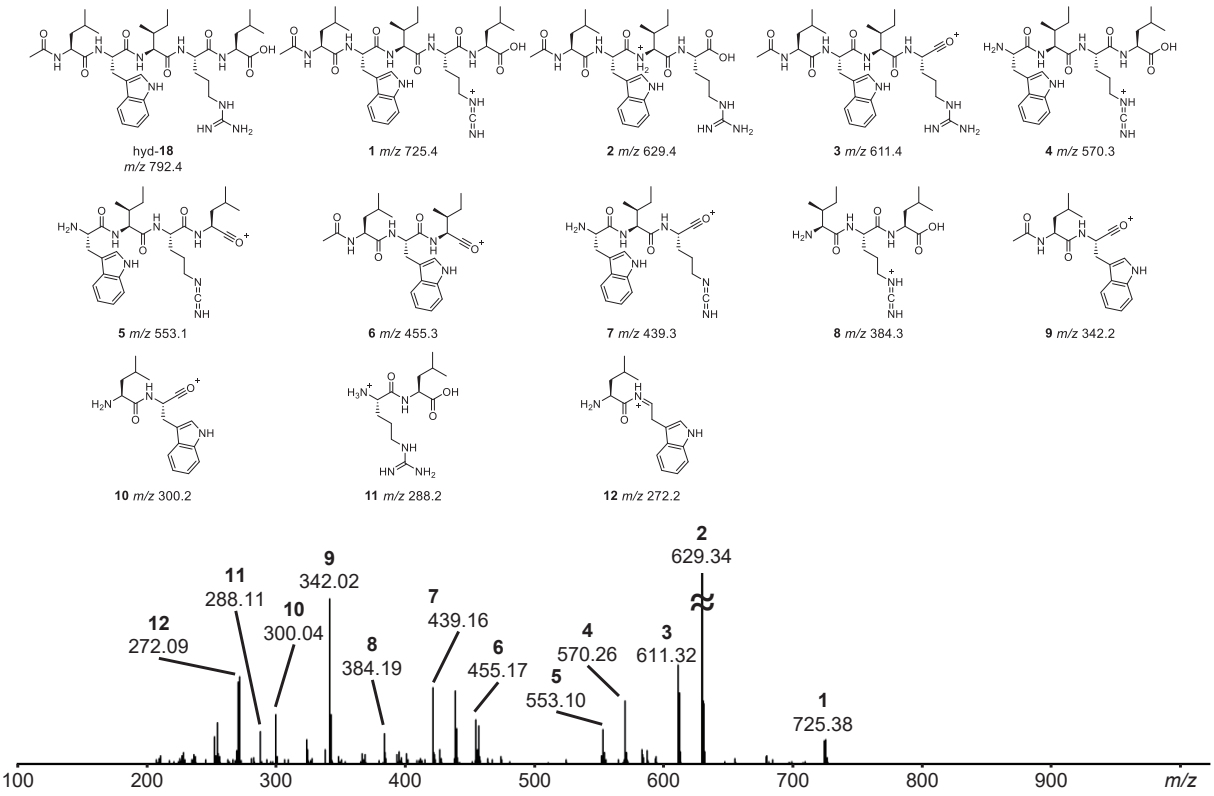

Figure S27. MS2 spectrum of hyd-**18**

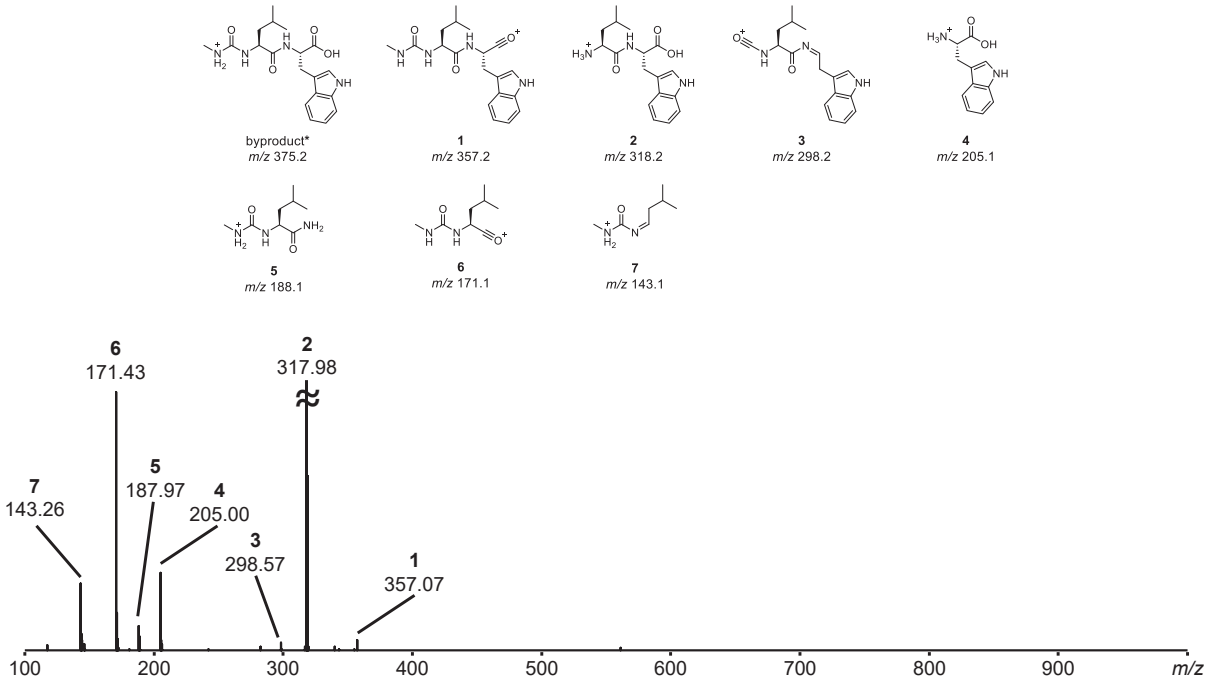

Figure S28. MS2 spectrum of the byproduct* shown in Figure 3h.

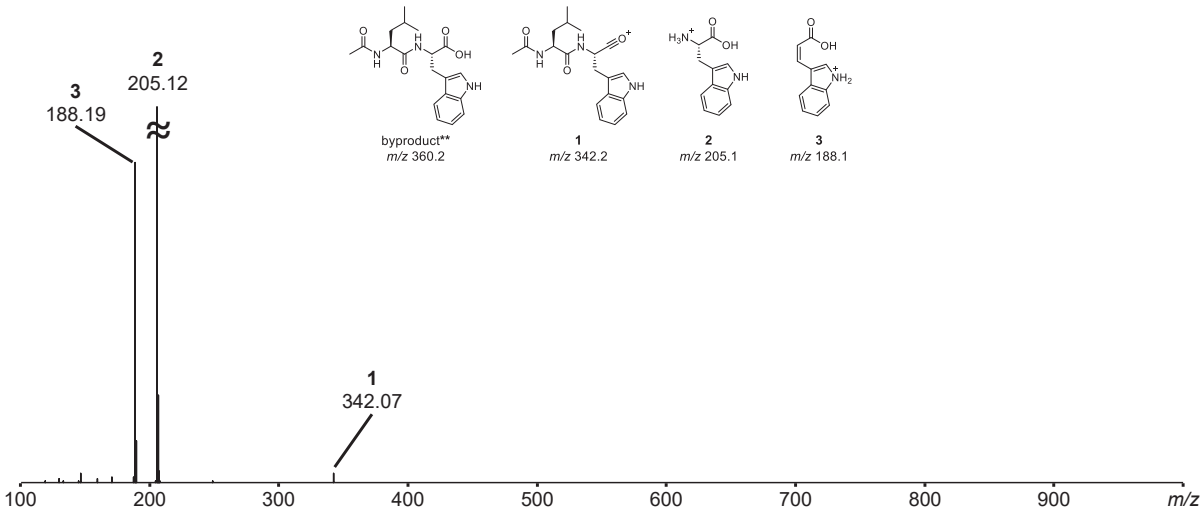

Figure S29. MS2 spectrum of the byproduct** shown in Figure 3i.

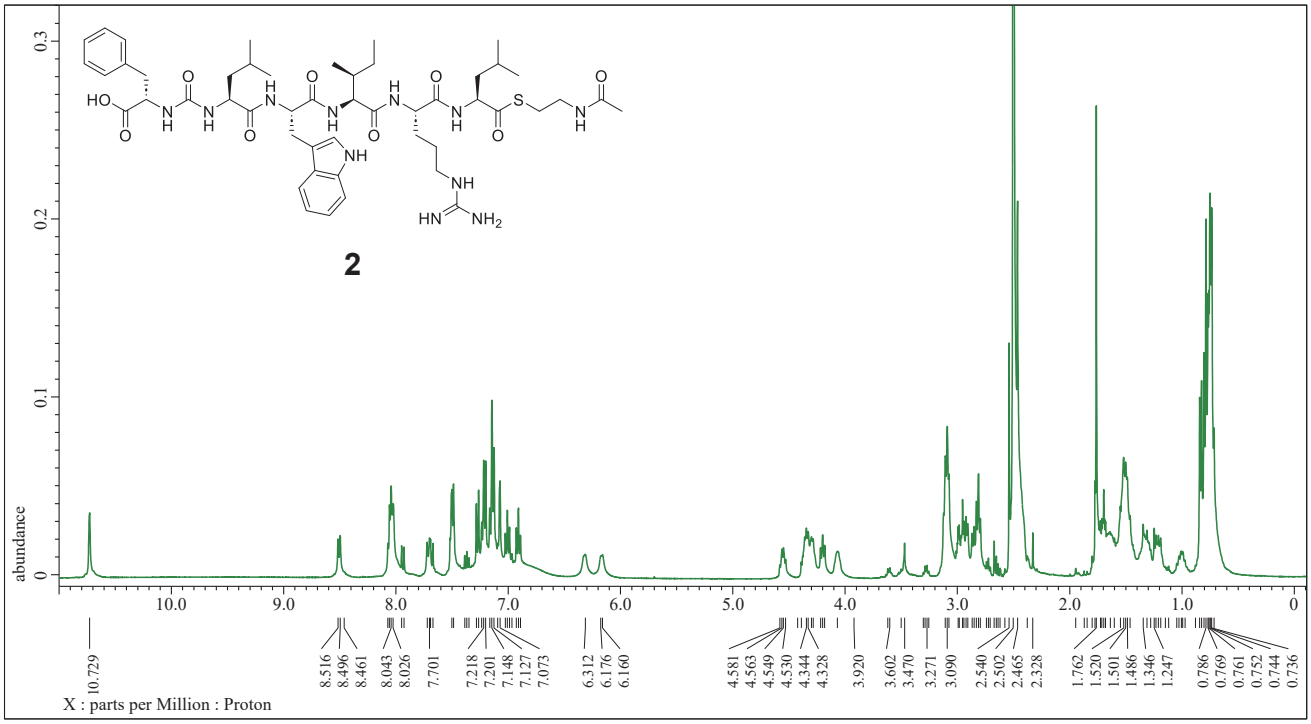

Figure S30. ^{1}H NMR spectrum of *seco*-bulbiferamide-SNAC (**2**) in DMSO-d_6 (400 MHz)

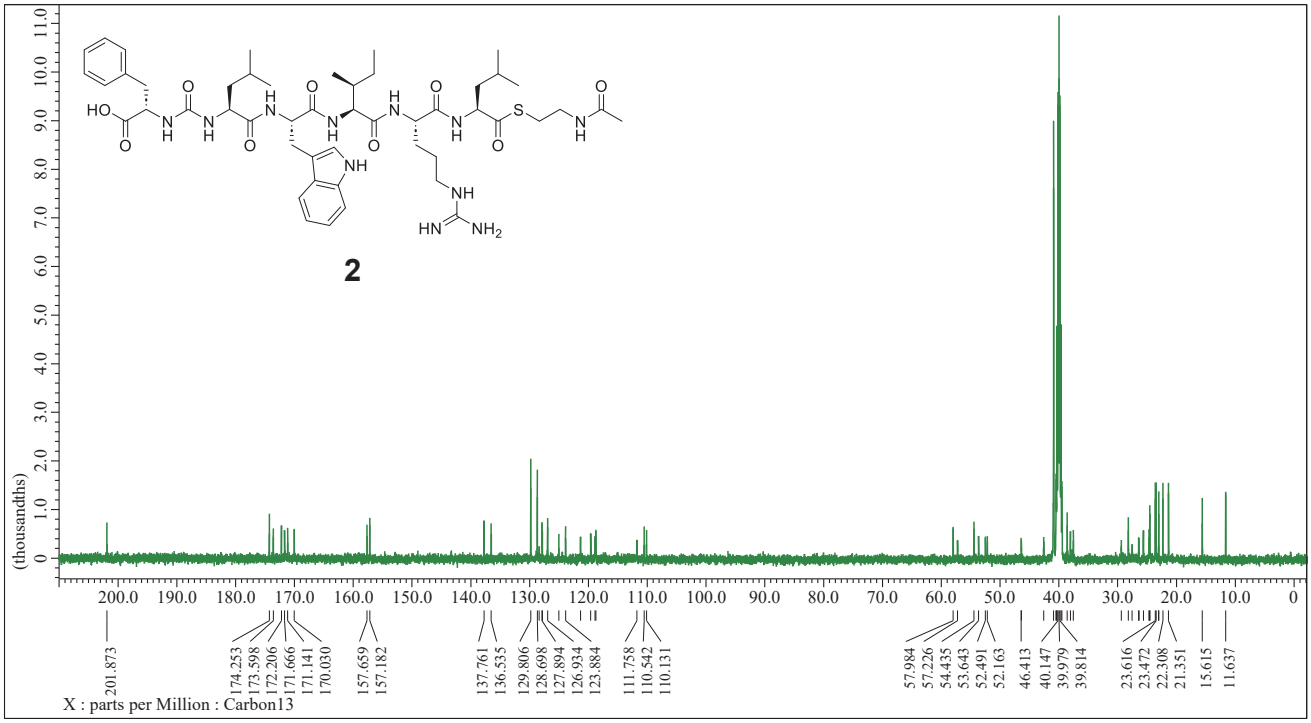

Figure S31. ^{13}C NMR spectrum of *seco*-bulbiferamide-SNAC (**2**) in DMSO-d_6 (100 MHz)

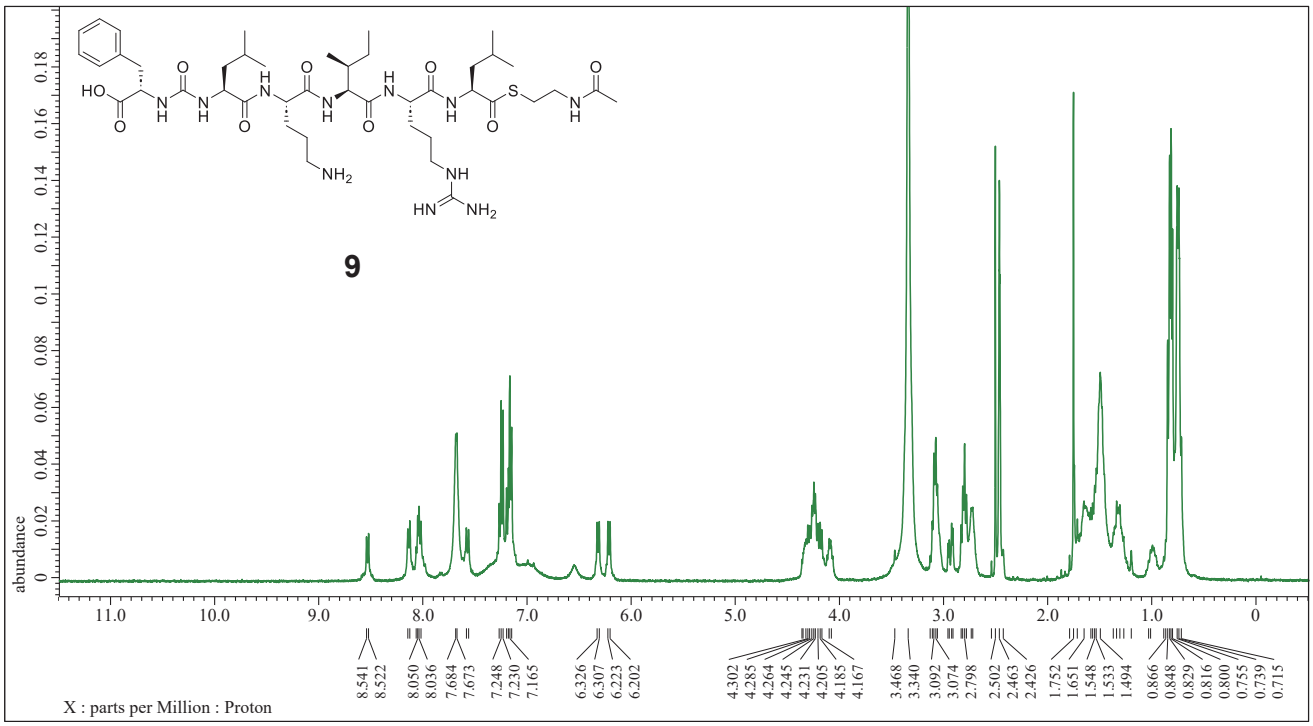

Figure S32. ^{1}H NMR spectrum of *seco*-bulbiferamide(W3O)-SNAC (**9**) in DMSO-d_6 (400 MHz)

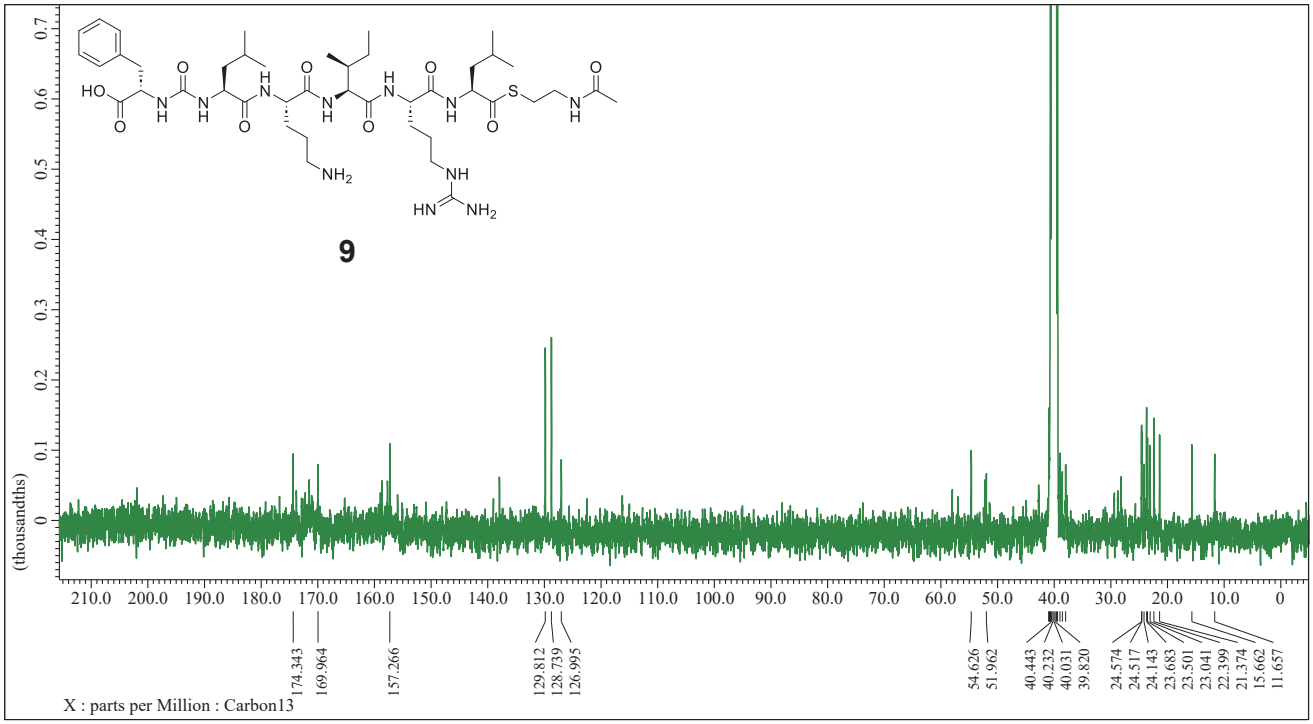

Figure S33. ^{13}C NMR spectrum of *seco*-bulbiferamide(W3O)-SNAC (**9**) in DMSO-d_6 (100 MHz)

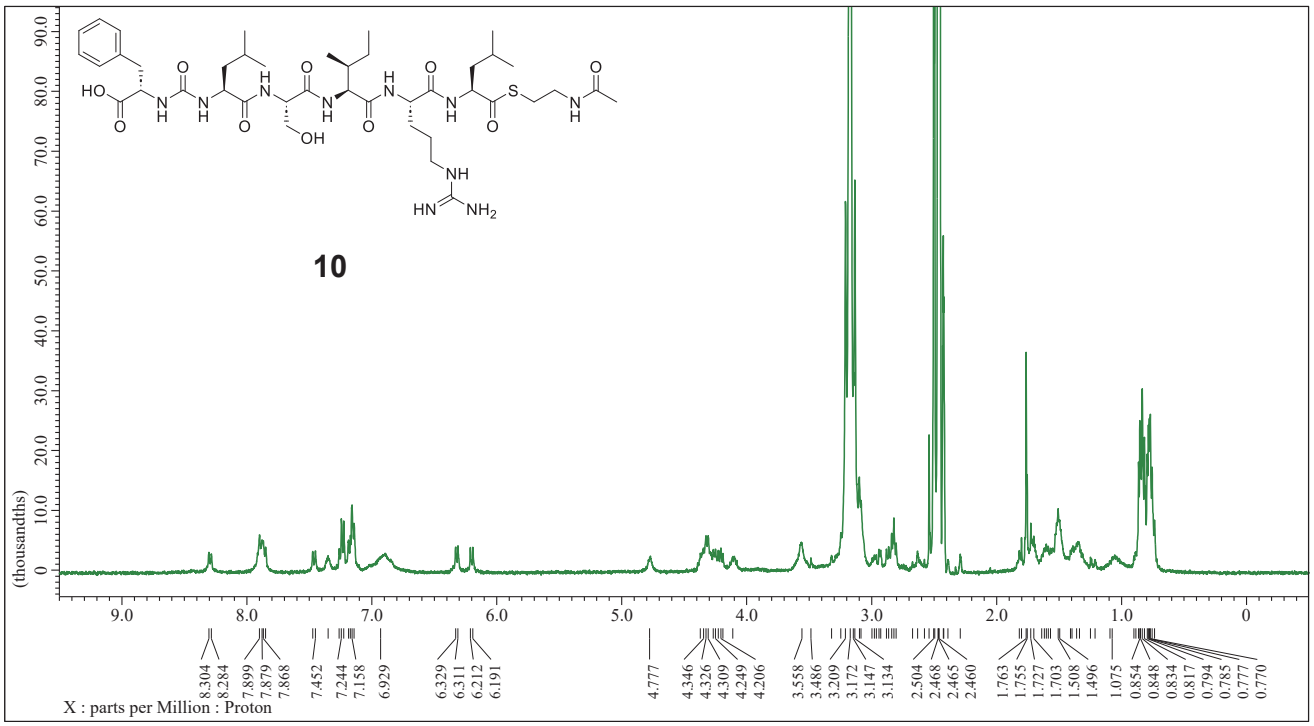

Figure S34. ^{1}H NMR spectrum of *seco*-bulbiferamide(W3S)-SNAC (**10**) in DMSO-d_6 (500 MHz)

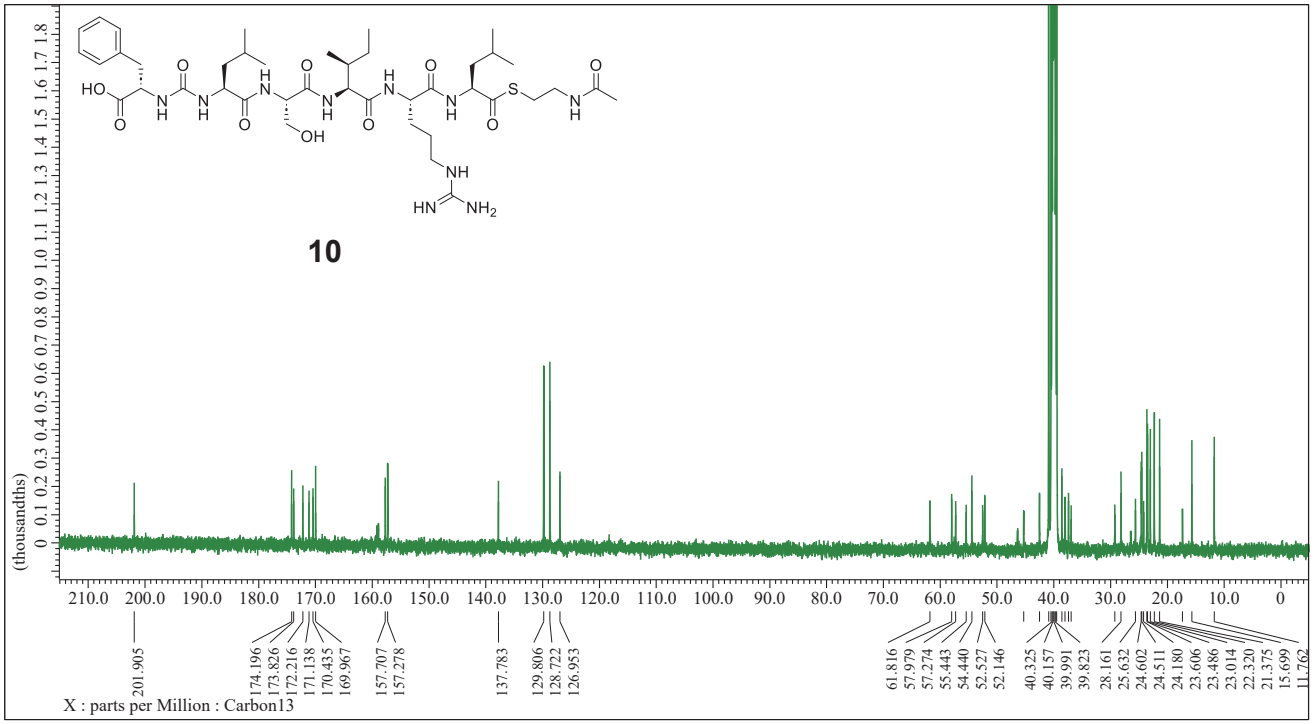

Figure S35. ^{13}C NMR spectrum of *seco*-bulbiferamide(W3S)-SNAC (**10**) in DMSO-d_6 (125 MHz)

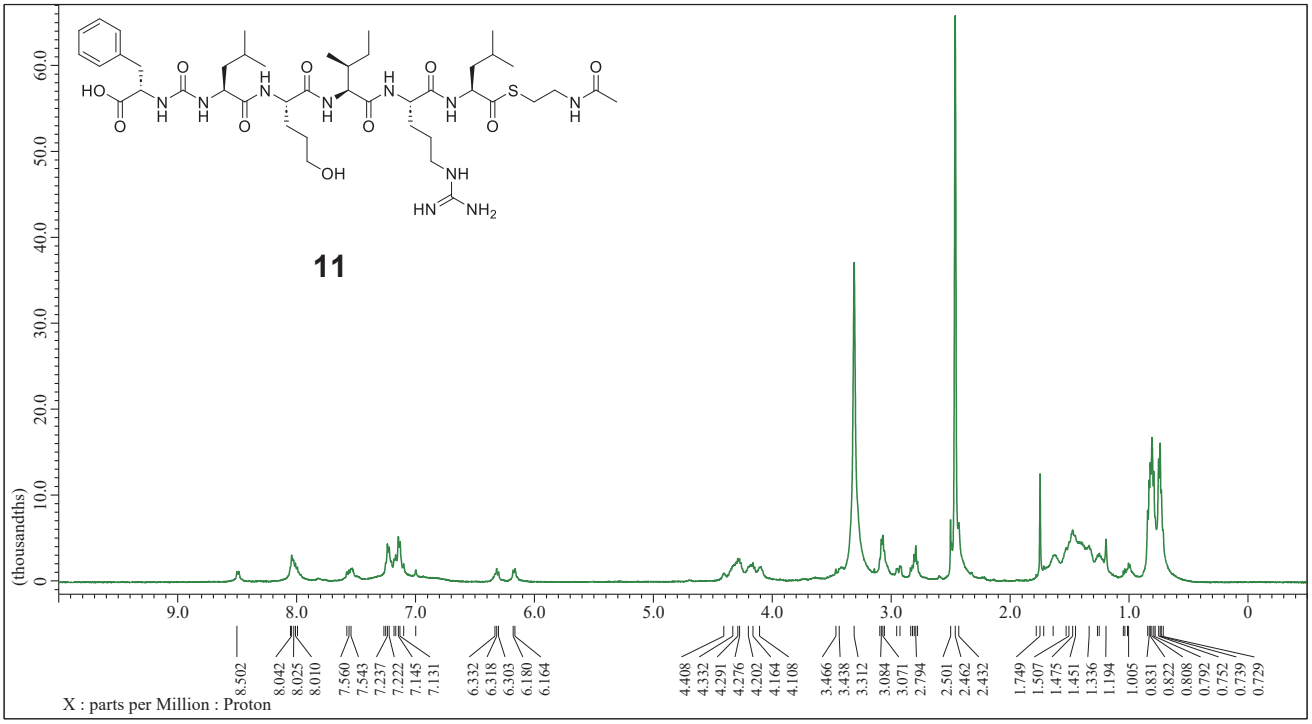

Figure S36. ^{1}H NMR spectrum of *seco*-bulbiferamide(W3Nva5-OH)-SNAC (**11**) in DMSO-d_6 (500 MHz)

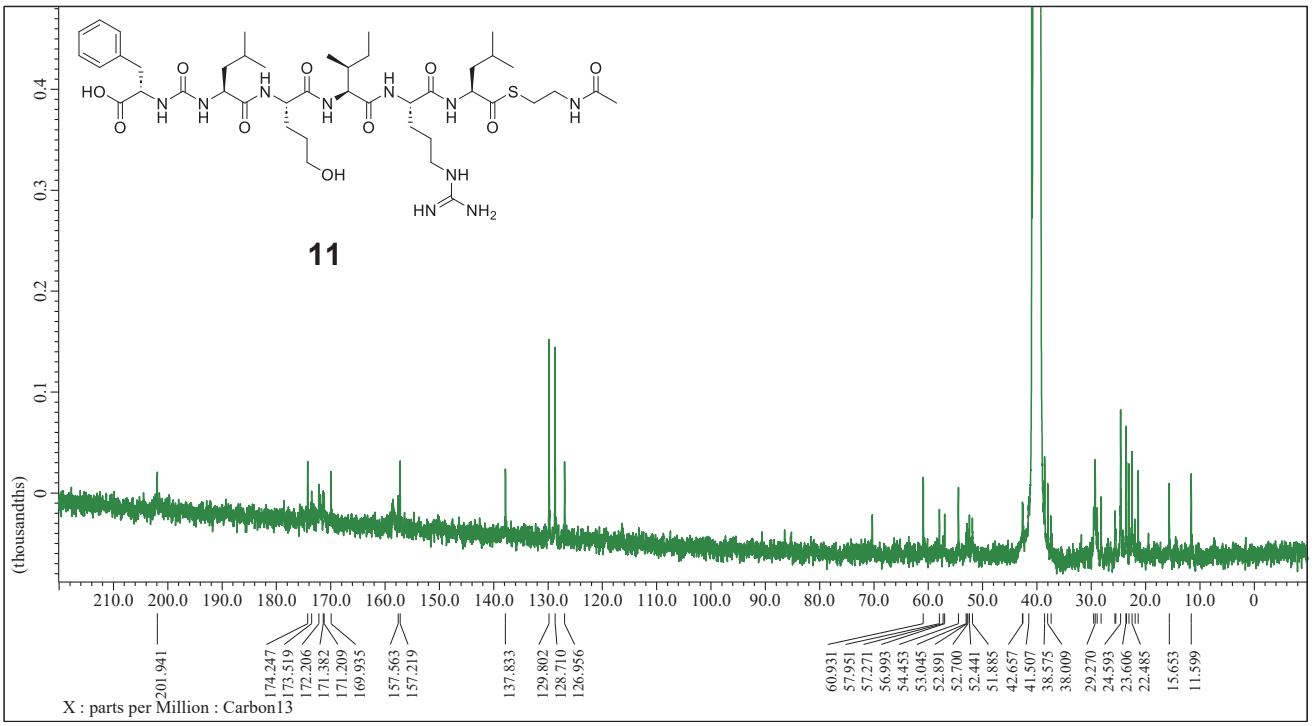

Figure S37. ^{13}C NMR spectrum of *seco*-bulbiferamide(W3Nva5-OH)-SNAC (**11**) in DMSO-d_6 (125 MHz)

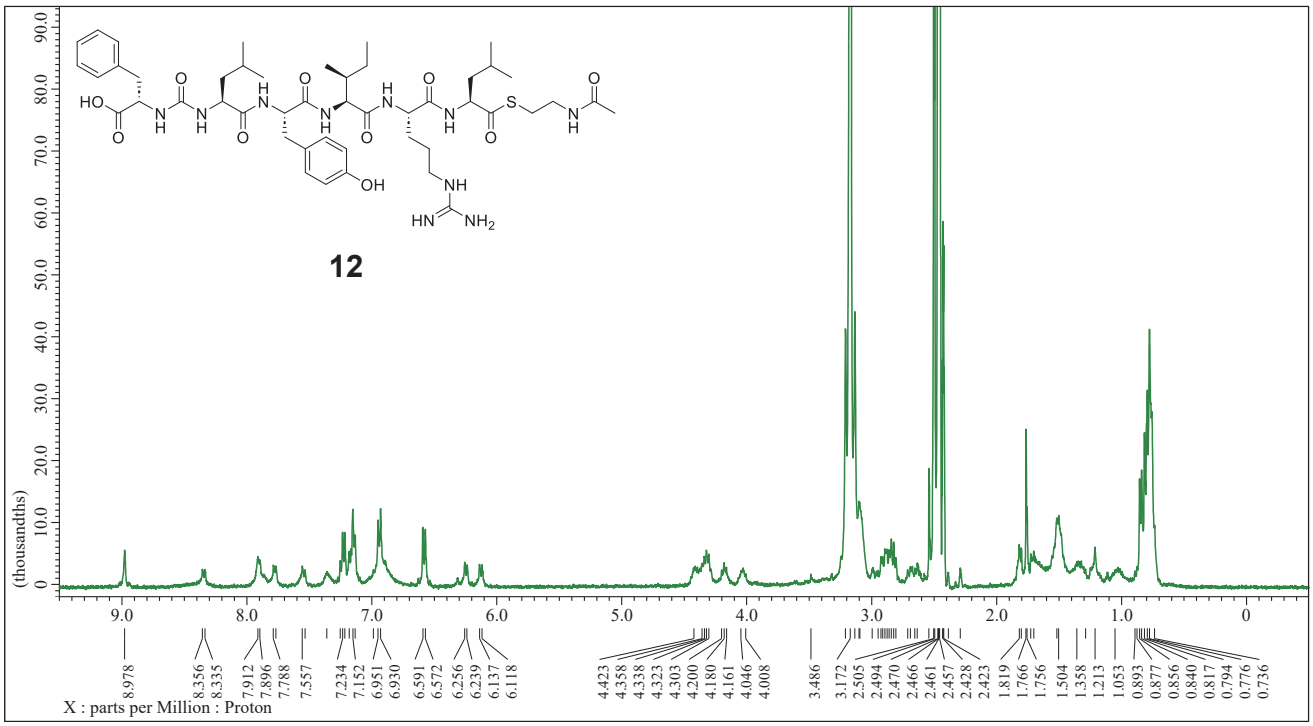

Figure S38. ^{1}H NMR spectrum of *seco*-bulbiferamide(W3Y)-SNAC (**12**) in DMSO-d_6 (500 MHz)

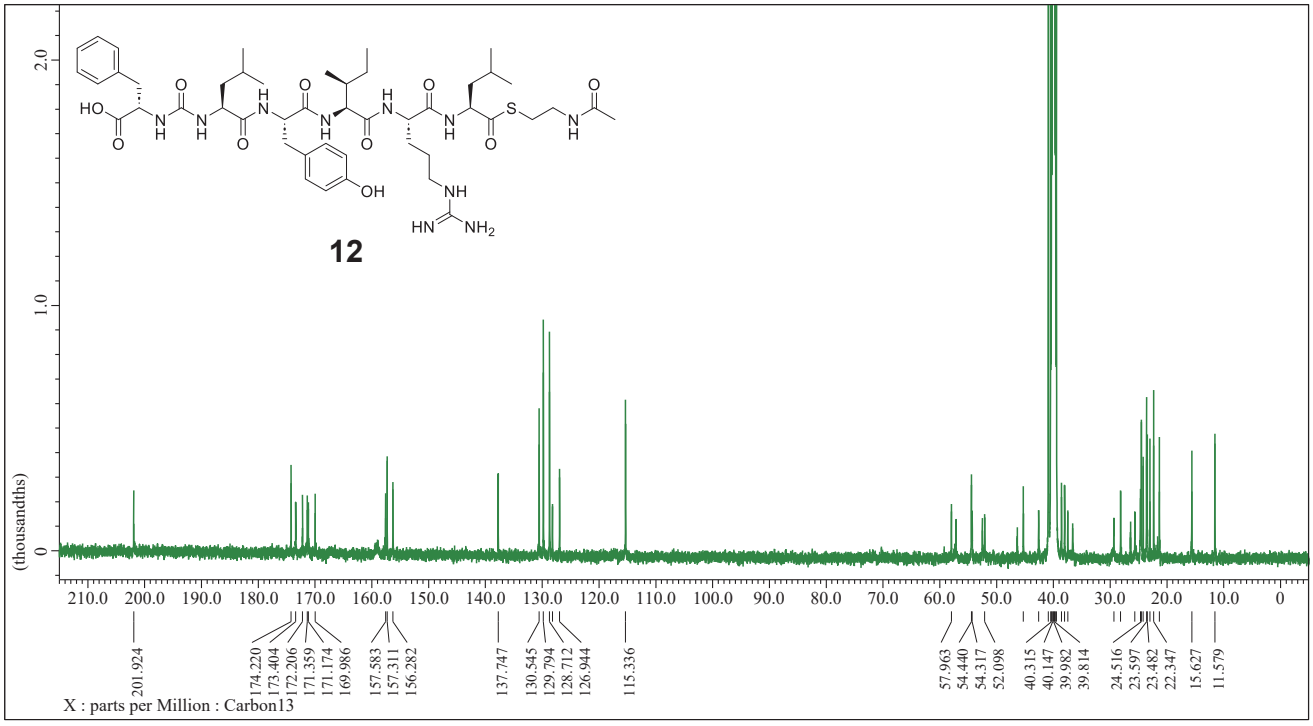

Figure S39. ^{13}C NMR spectrum of *seco*-bulbiferamide(W3Y)-SNAC (**12**) in DMSO-d_6 (125 MHz)

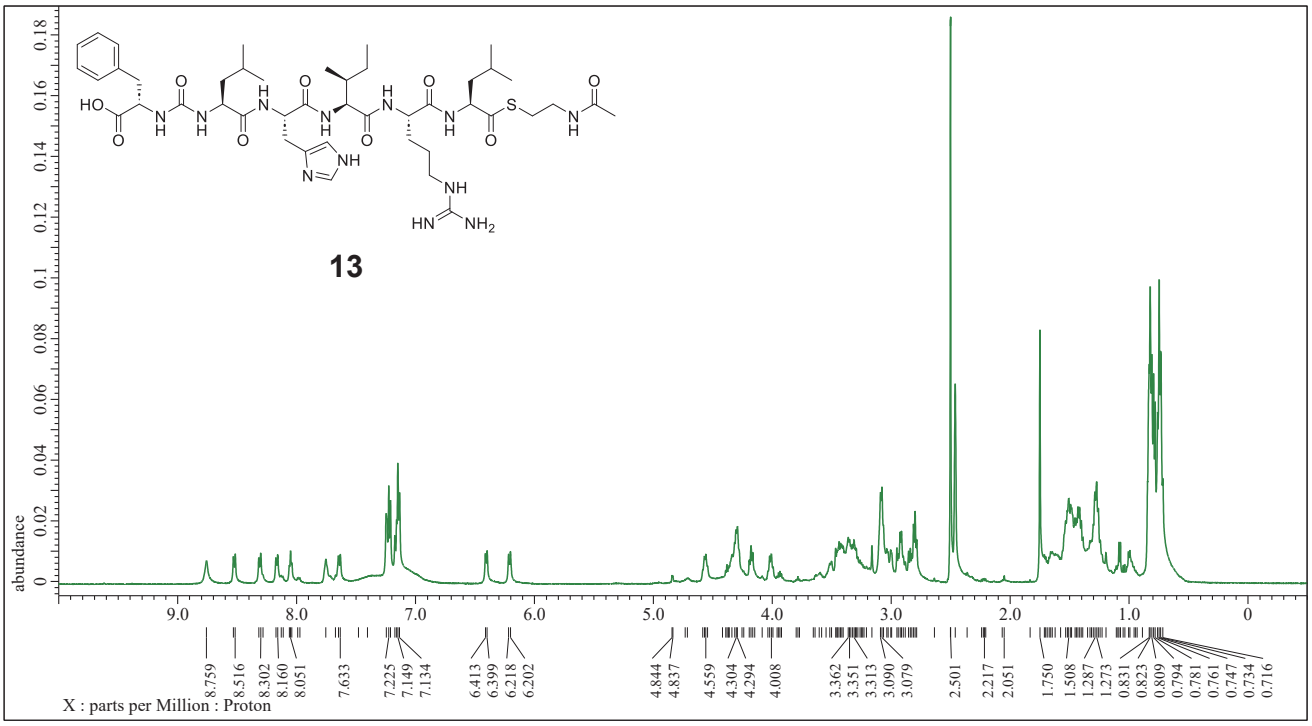

Figure S40. ^{1}H NMR spectrum of *seco*-bulbiferamide(W3H)-SNAC (**13**) in DMSO-d_6 (500 MHz)

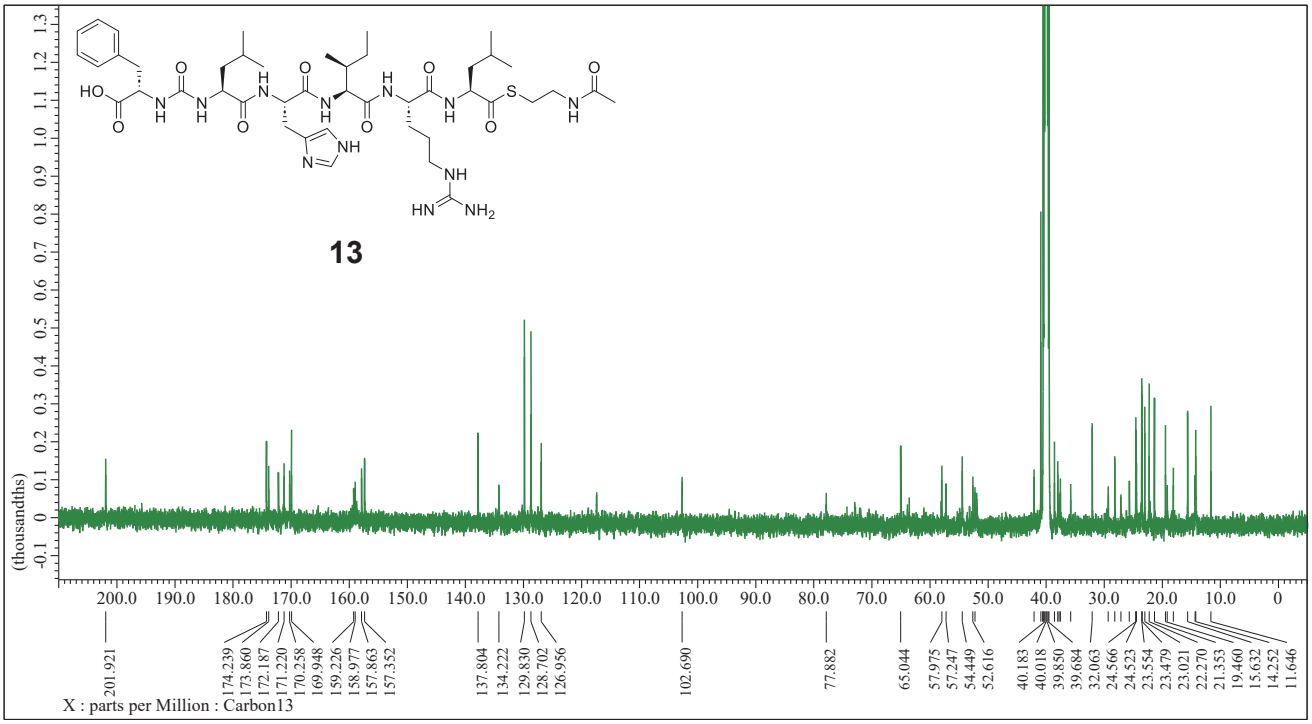

Figure S41. ^{13}C NMR spectrum of *seco*-bulbiferamide(W3H)-SNAC (**13**) in DMSO-d_6 (125 MHz)

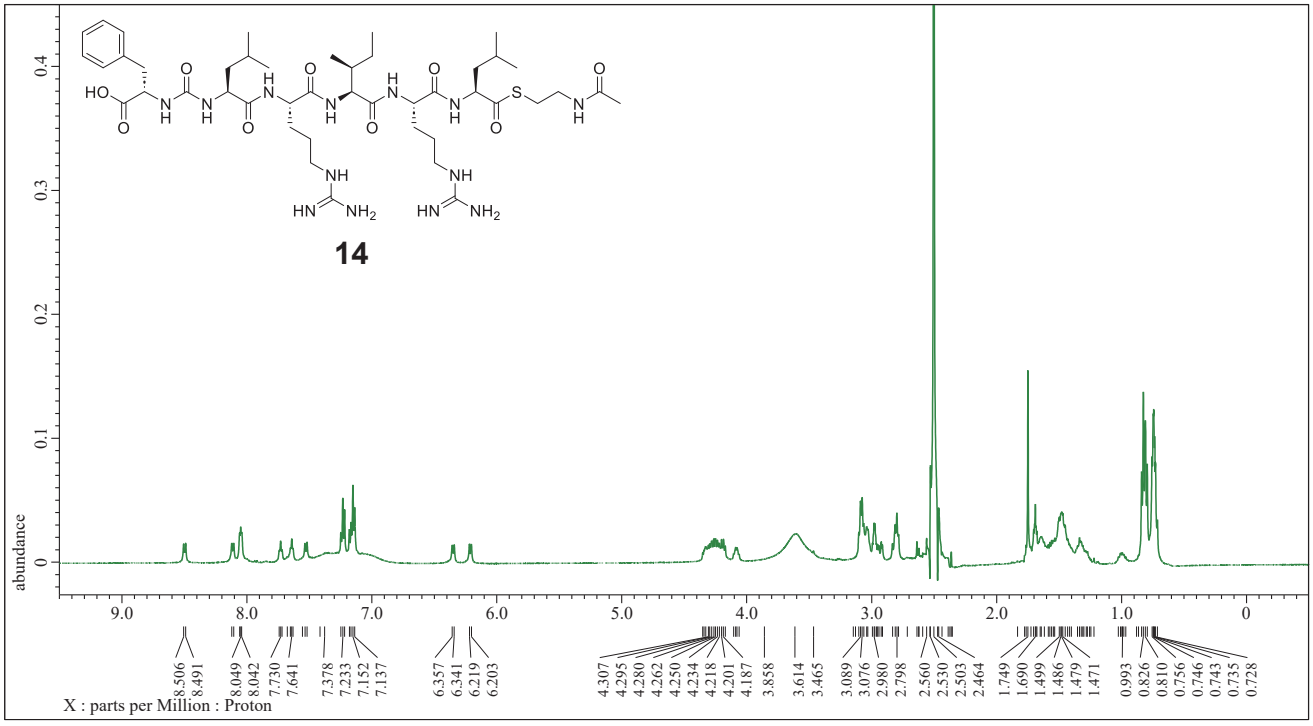

Figure S42. ^{1}H NMR spectrum of *seco*-bulbiferamide(W3R)-SNAC (**14**) in DMSO-d_6 (500 MHz)

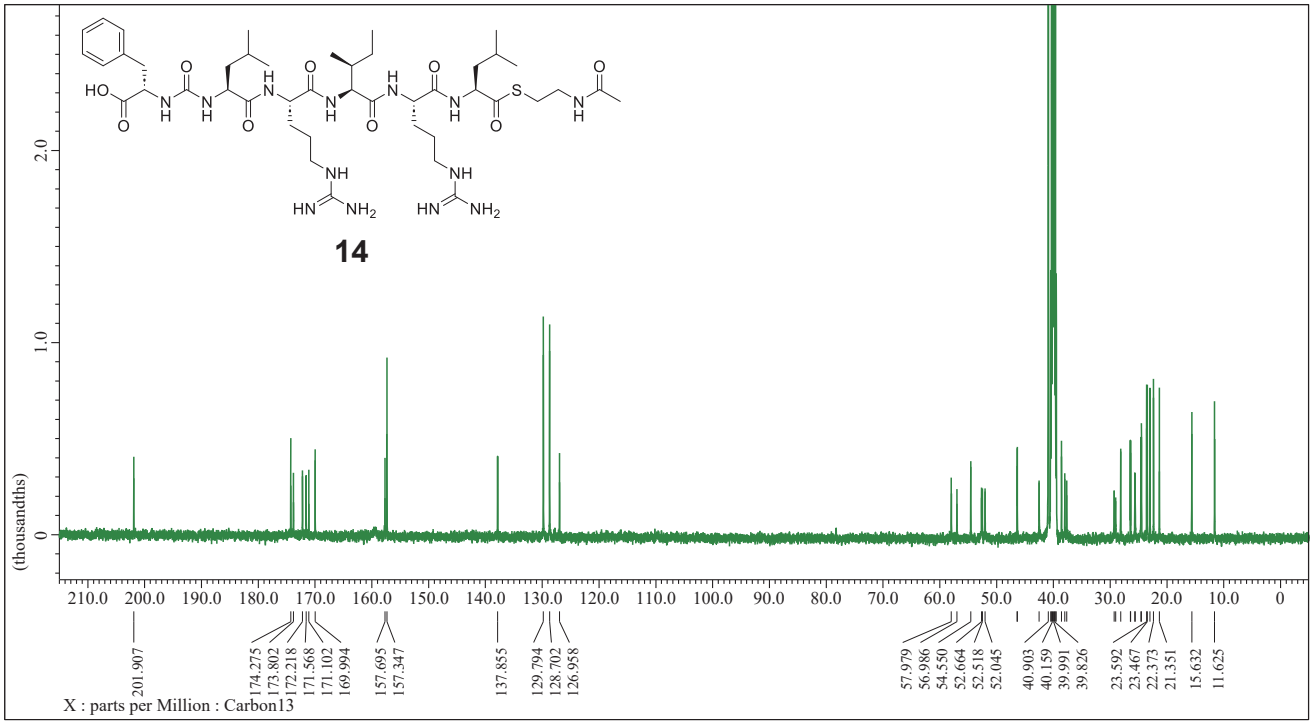

Figure S43. ^{13}C NMR spectrum of *seco*-bulbiferamide(W3R)-SNAC (**14**) in DMSO-d_6 (125 MHz)

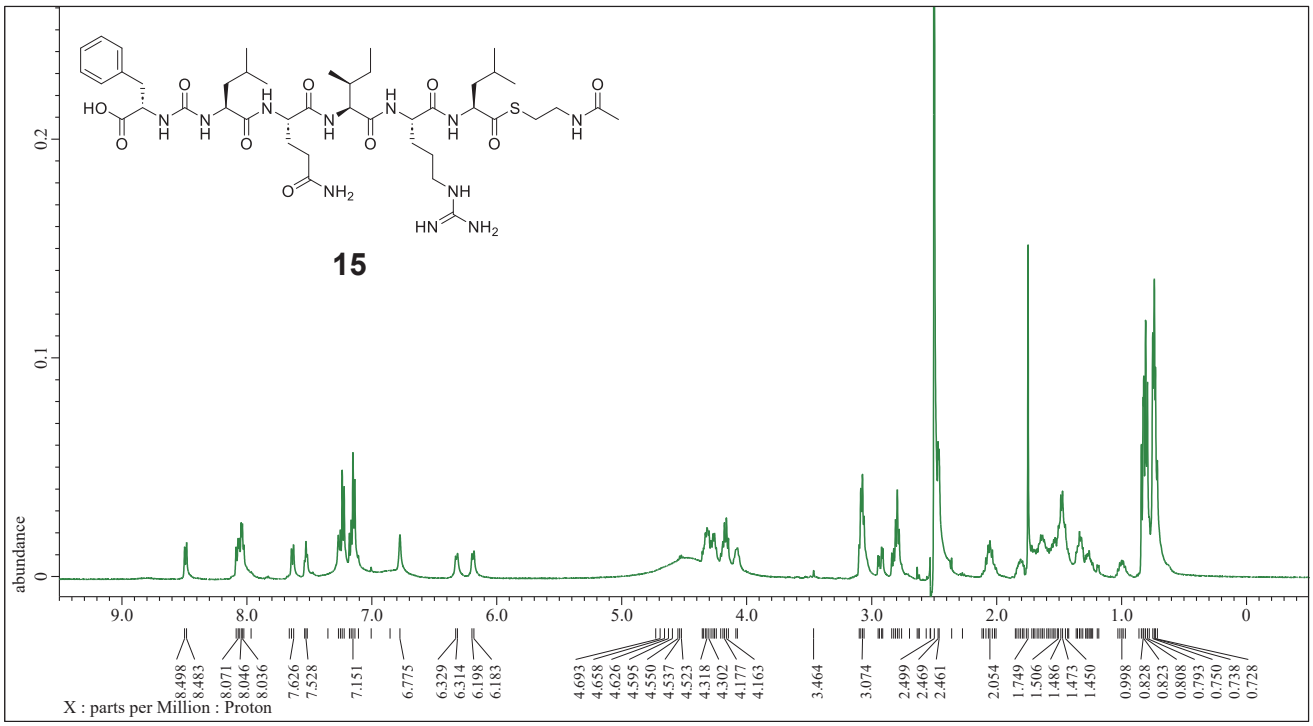

Figure S44. ^{1}H NMR spectrum of *seco*-bulbiferamide(W3N)-SNAC (**15**) in DMSO-d_6 (400 MHz)

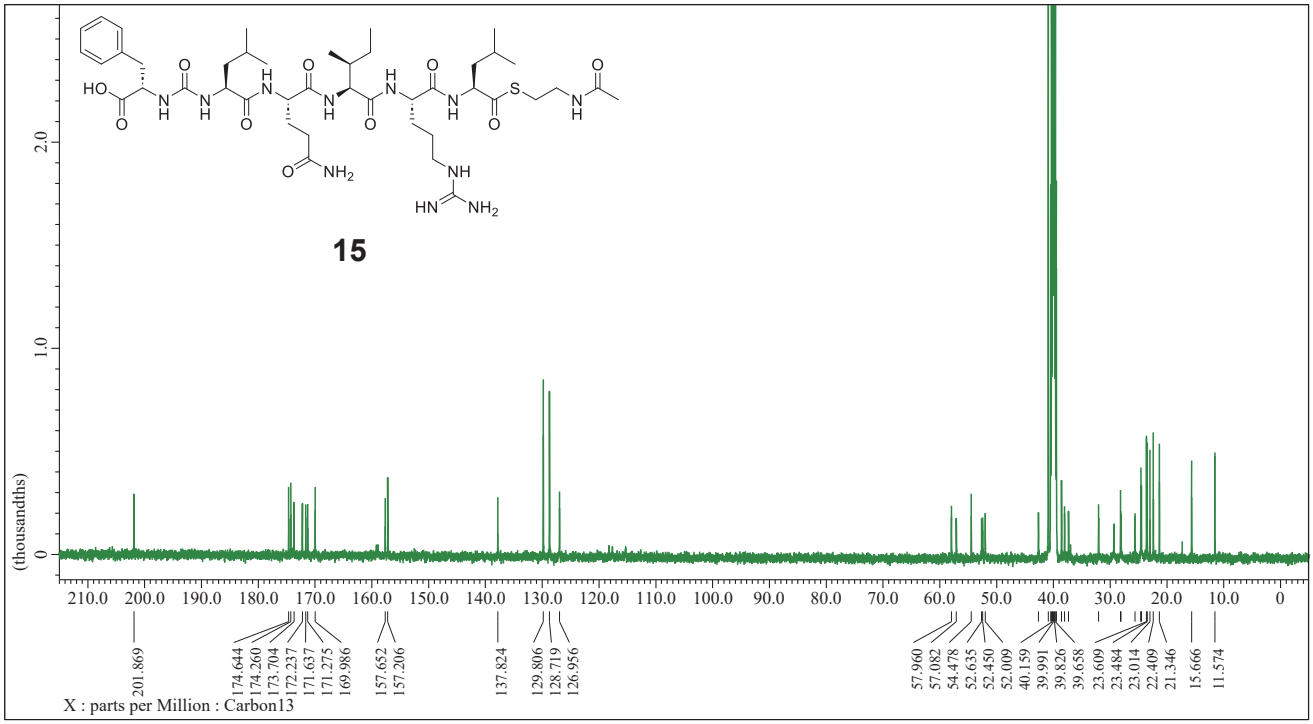

Figure S45. ^{13}C NMR spectrum of *seco*-bulbiferamide(W3N)-SNAC (**15**) in DMSO-d_6 (100 MHz)

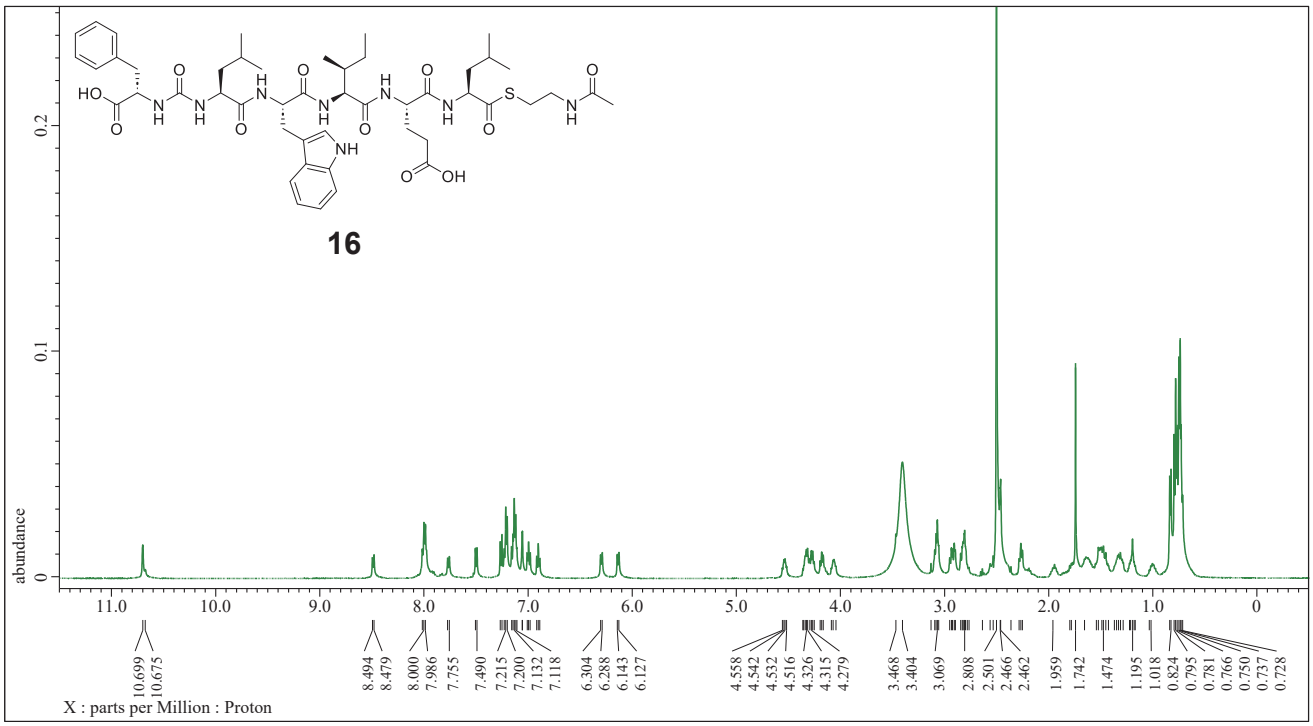

Figure S46. ^{1}H NMR spectrum of *seco*-bulbiferamide(W5E)-SNAC (**16**) in DMSO-d_6 (500 MHz)

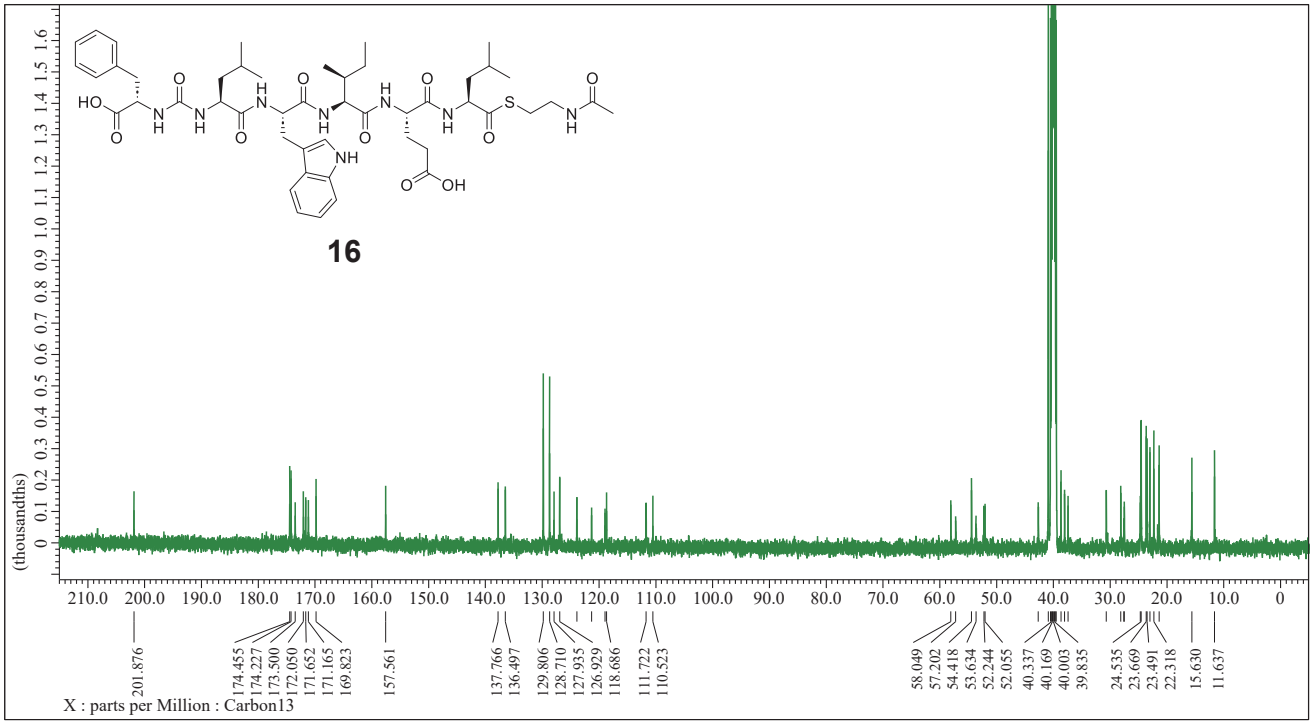

Figure S47. ^{13}C NMR spectrum of *seco*-bulbiferamide(W5E)-SNAC (**16**) in DMSO-d_6 (125 MHz)

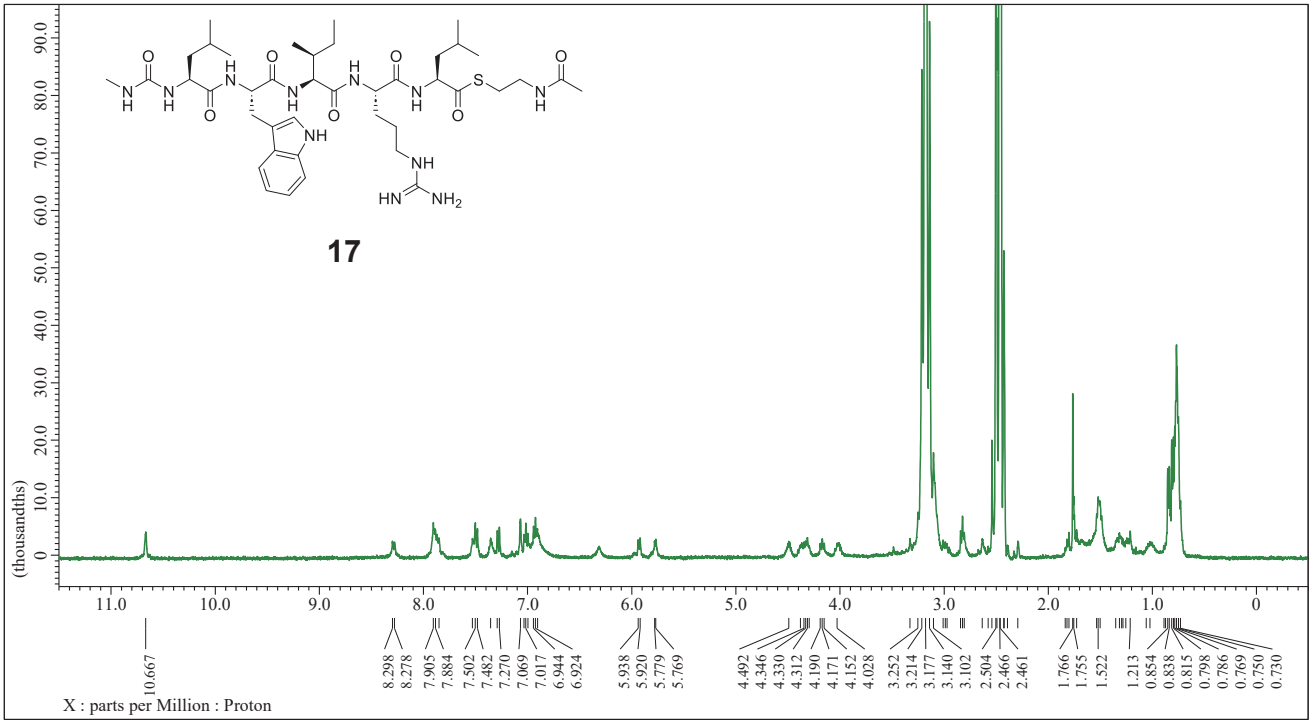

Figure S48. ^{1}H NMR spectrum of *seco*-bulbiferamide(F1Me)-SNAC (**17**) in DMSO-d_6 (500 MHz)

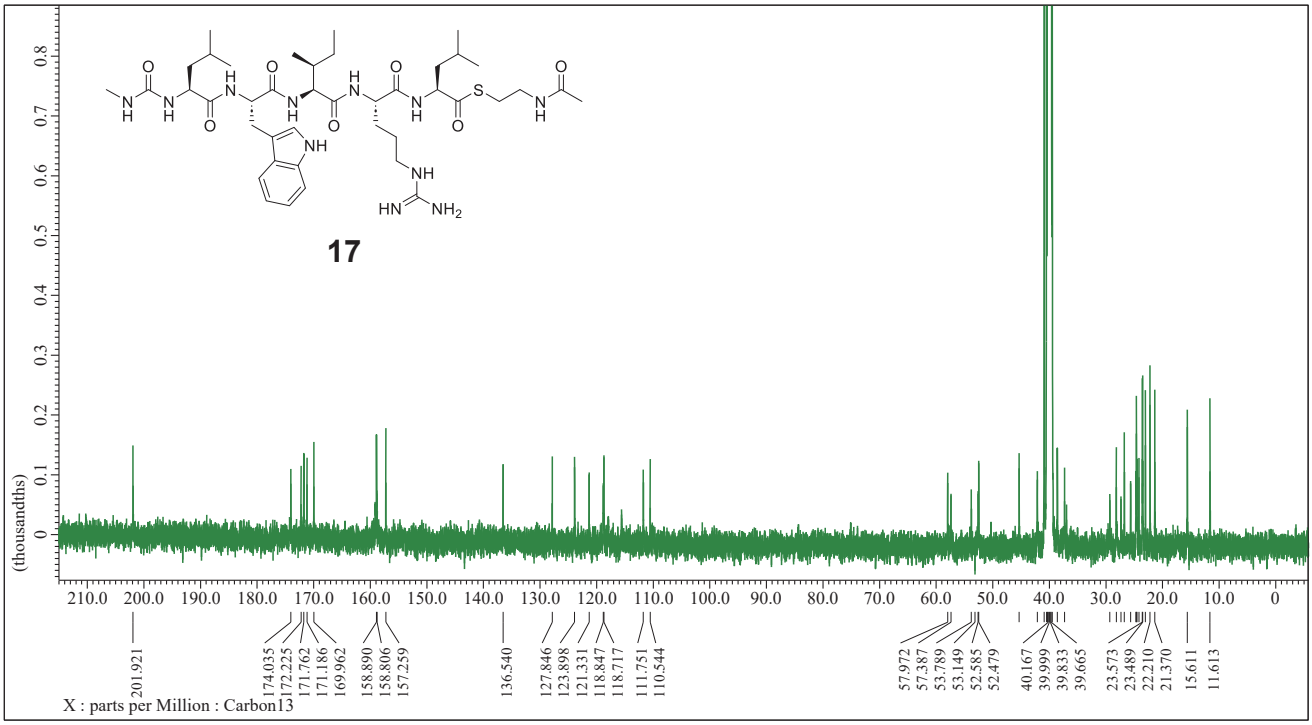

Figure S49. ^{13}C NMR spectrum of *seco*-bulbiferamide(F1Me)-SNAC (**17**) in DMSO-d_6 (125 MHz)

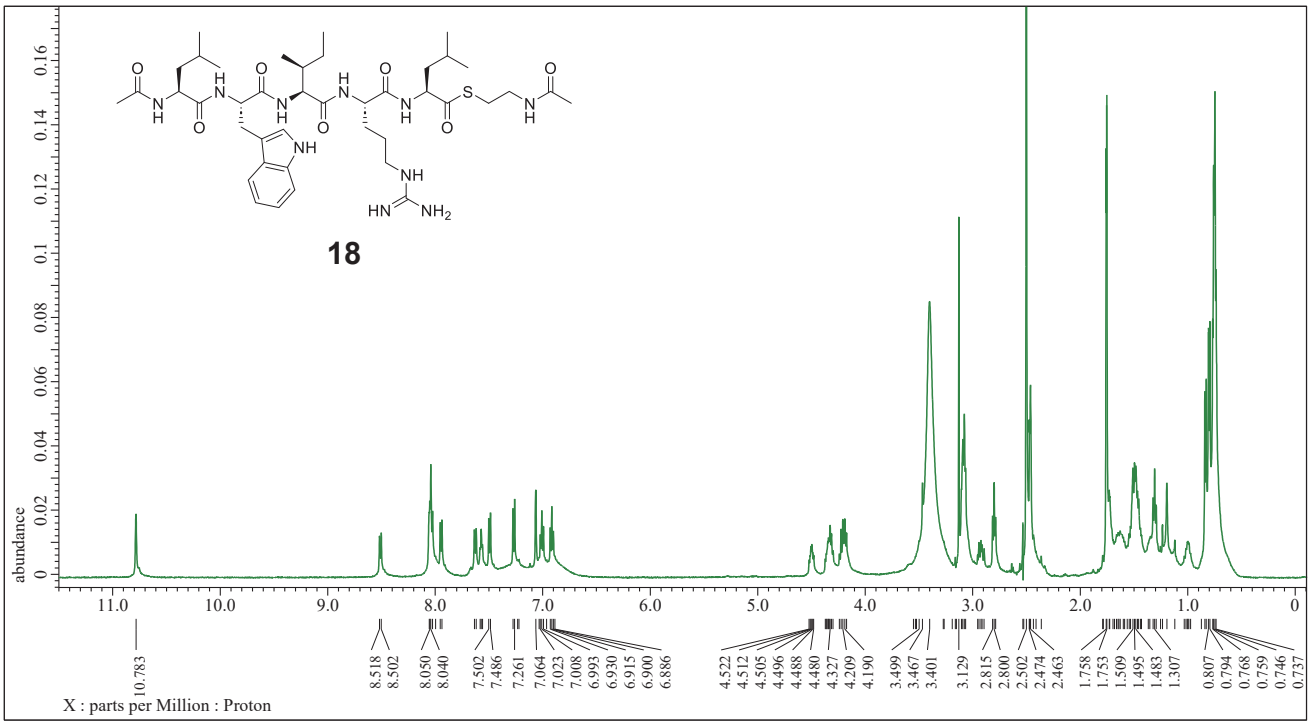

Figure S50. ^{1}H NMR spectrum of *seco*-*N*-acetyl bulbiferamide-SNAC (**18**) in DMSO-d_6 (500 MHz)

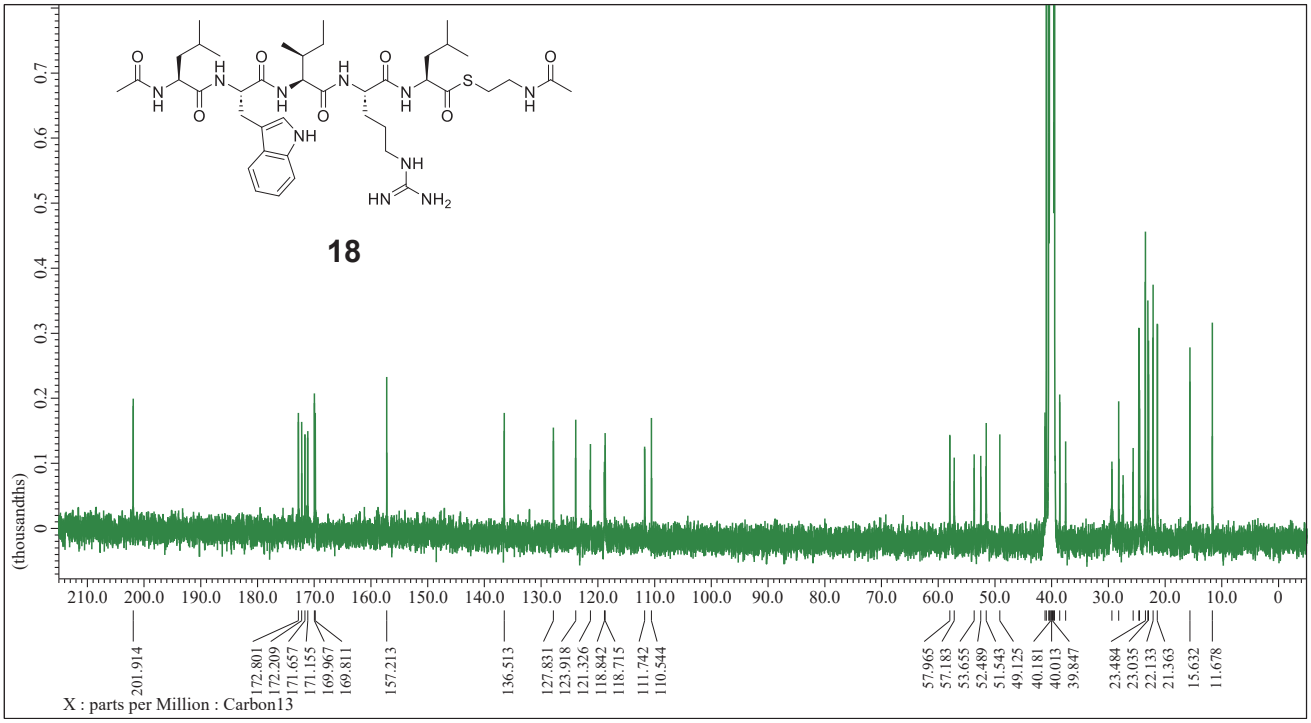

Figure S51. ^{13}C NMR spectrum of *seco*-*N*-acetyl bulbiferamide-SNAC (**18**) in DMSO-d_6 (125 MHz)

References

[1] J. Jumper, R. Evans, A. Pritzel, T. Green, M. Figurnov, O. Ronneberger, K. Tunyasuvunakool, R. Bates, A. Žídek, A. Potapenko, A. Bridgland, C. Meyer, S. A. A. Kohl, A. J. Ballard, A. Cowie, B. Romera-Paredes, S. Nikolov, R. Jain, J. Adler, T. Back, S. Petersen, D. Reiman, E. Clancy, M. Zielinski, M. Steinegger, M. Pacholska, T. Berghammer, S. Bodenstein, D. Silver, O. Vinyals, A. W. Senior, K. Kavukcuoglu, P. Kohli, D. Hassabis, *Nature* **2021**, *596*, 583–589.

[2] H. Knolker, T. Braxmeier, *Syn. Lett.* **1997,** *8*, 925–928.

[3] Y. M. Elbatrawi, C. W. Kang, J. R. D. Valle, *Org. Lett.* **2018,** *20*, 2707–2210.

[4] J. Eberhardt, D. Santos-Martins, A. F. Tillack, S. Forli, *J. Chem. Inf. Model.* **2021**, *61*, 3891–3898.

[5] S. Lu, Z. Zhang, A. R. Sharma, J. Nakajima-Shimada, E. Harunari, N. Oku, A. Trianto, Y. Igarashi, Y. *J. Nat. Prod.* **2023**, *86*, 1081–1086.

[6] D. A. Case, H. M. Aktulga, K. Belfon, D. S. Cerutti, G. A. Cisneros, V. W. D. Cruzeiro, N. Forouzesh, T. J. Giese, A. W. Götz, H. Gohlke, S. Izadi, K. Kasavajhala, M. C. Kaymak, E. King, T. Kurtzman, T.-S. Lee, P. Li, J. Liu, T. Luchko, R. Luo, M. Manathunga, M. R. Machado, H. M. Nguyen, K. A. O'Hearn, A. V. Onufriev, F. Pan, S. Pantano, R. Qi, A. Rahnamoun, A. Risheh, S. Schott-Verdugo, A. Shajan, J. Swails, J. Wang, H. Wei, X. Wu, Y. Wu, S. Zhang, S. Zhao, Q. Zhu, T. E. I. Cheatham, D. R. Roe, A. Roitberg, C. Simmerling, D. M. York, M. C. Nagan, K. M. Jr. Merz, *J. Chem. Inf. Model.* **2023**, *63*, 6183–6191.

[7] Y. Moriwaki, T. Terada, J. M. Caaveiro, Y. Takaoka, I. Hamachi, K. Tsumoto, K. Shimizu, *Biochemistry* **2013**, *52*, 8866–8877.

[8] M. J. Abraham, T. Murtola, R. Schulz, S. Páll, J. C. Smith, B. Hess, E. Lindahl, *SoftwareX* **2015**, *1*, 19–25.

[9] A. Berger, K. Valant-Vetschera, J. Schinnerl, L. Brecker, *Phytochem. Rev.* **2022**, *21*, 915–939.

[10] Y. Fu, Y. Zhang, H. He, L. Hou, Y. Di, S. Li, X. Luo, X. Hao, *J. Nat. Prod.* **2012**, *75*, 1987–1990.

[11] W. L. Liang, X. Le, H. J. Li, X. L. Yang, J. X. Chen, J. Xu, H. L. Liu, L. Y. Wang, K. T. Wang, K. C. Hu, D. P. Yang, W. J. Lan, *Mar. Drugs* **2014**, *12*, 5657–5676.

[12] M. Zhao, H. C. Lin, Y. Tang, *J. Antibiot.* **2016**, *69*, 571-573.

[13] W. Zhong, J. M. Deutsch, D. Yi, N. H. Abrahamse, I. Mohanty, S. G. Moore, A. C. McShan, N. Garg, V. Agarwal, *ChemBioChem*. **2023**, *24*, e202300190

[14] H. J. Imker, C. T. Walsh, W. M. Wuest, *J. Am. Chem. Soc.* **2009,** *131*, 18263–18265.

[15] C. L. M. Gilchrist, M. Mirdita, M. Steinegger, *bioRxiv preprint* **2024**, DOI: 10.1101/2024.08.01.606130.

[16] X. Robert, P. Gouet, *Nucl. Acids Res.* **2014**, *42*, W320–W324.